Probable physical factors of anthropogenesis

Alexander Kholmanskiy

Moscow State University of Medicine and Dentistry

allexhol@ya.ru, https://orcid.org/0000-0001-8738-0189

Abstract

The increasing frequency of climate catastrophes worldwide against background of global warming and reduction of biodiversity in human ecosystem are typical signs of global extinction, the sixth in ~600 million years of Phanerozoic. The regularity of global extinctions of marine biota with a period of ~62 Myr in Phanerozoic correlates with cyclicity of tidal effects of stellar environment of Solar System as it revolves around center of Galaxy. In accordance with Anthropic Principle, abiogenic factors of mass extinctions can correct evolution along vector of anthropogenesis. Human parasitism on biosphere, demographic problems and stagnation of sapientation during 6th extinction suggest launch of mutagenesis, necessary for fixing dominance of thinking over the instinct of reproduction at level of the human genome. Taking into account chirality of bilaterals, sexual dimorphism and molecular mechanism of circadian clock, it was suggested that role of mutagenic factor is played by chiral photon-neutrino quanta, genetically linked to the neutrino of the proton-proton cycle of Sun's energy. Sensitization of biosphere to action of chiral factor at night will be provided by anomalous physicochemical properties of liquid water in hydrosphere and in physiological fluids. It is shown that the ~11-year cycle of Solar activity reflects the influence on the physics of Sun of periodicity of the tidal effects of syzygy of Jupiter, Venus and Earth, as well as interactions of magnetic dipoles of Sun and Jupiter. Synchronous with Solar activity changes in flux of chiral quanta on the night side of earth will be additionally modulated by geography and this will manifest itself in differences in mentality of population of southern and northern hemispheres of Earth, as well as coastal and continental territories.

Key words: Galaxy, Sun, planets, biosphere, chirality, water, temperature, mutagenesis.

1. Introduction

The very fact of the emergence of intelligent life on Earth testifies to coordinated and purposeful action of cosmic and geophysical factors at all stages of the evolution of biosphere. This pattern allows us to expand the forms of implementation of the Anthropic principle to the molecular-cellular level of self-organization of matter. Functionally and morphologically, physiology of plants and animals reflects participation of elemental base of all geospheres and geophysics in processes of self-organization and development of heterochiral living systems under the influence of biogenic solar radiation [Kholmanskiy, 2019]. The key role in these processes was played by unique physicochemical properties of water in the hydrosphere and physiological fluids at a temperature (T)

from ~0 to ~42 °C [Eisenberg, 2007; Kholmanskiy, 2023], as well as prebiotic synthesis of right-handed ribose, the structural basis of ATP, RNA and DNA molecules [Parmon, 2008; Kholmanskiy, 2016]. The synergism of biogenic solar radiation on the day and night sides of Earth determined the development at molecular level of a mechanism for subordinating living systems to a circadian rhythm, which is manifested in the electrophysics and thermodynamics of signaling and trophic communications of living organisms, from plants to humans [Kizel, 1985; Michel, 2019; Kholmanskiy, 2019; 2023a]. Optimization and genetic differentiation of the physiology of living organisms is provided by the energy-informational synergism of D-sugars and L-amino acids, which suggests the participation in bioenergetics along with achiral electromagnetic-gravitational component of a global chiral factor [Kholmanskiy, 2016; 2019; Globus, 2020]. In principle, solar electron neutrino (ν_e) is suitable for this role, since it has left-handed chirality (spin is opposite to momentum) and is formed in core of the Sun in reactions of proton-proton cycle, which form the basis of its energy [Borexino, 2018]. The relic form of neutrinos, in addition to relic photons, endows the space of Universe with chirality [Dolgov, 2008]. However, the existence of relic neutrinos has not yet been confirmed experimentally. Despite the fundamental nature and universality of neutrino physics, there is still no unambiguous confirmation of seasonal variations in high-energy solar neutrino fluxes and their influence on the rate of radioactive decay [Schirber, 2014; Maltoni, 2016; Picoreti, 2016; Athar, 2022; Delgado, 2022]. Moreover, the operating installations and neutrino telescopes, in principle, are not designed for direct registration of low-energy solar ν_e [Borexino, 2018].

In the works [Kholmanskiy, 2019; Picoreti, 2016], a hypothesis was put forward about instability of neutrinos and decay of ν_e into daughter chiral products (א-forms) in the core of the Sun. When leaving core into radiative zone, א-forms form hybrid neutrino-photon energy quanta with photons - אγ [Dolgov, 2008; Giunti, 2015]. The physical nature of א-forms is, in fact, similar to the nature of original dichotomous energy forms of matter, maximum number of which during decay of ν_e in a vacuum into relic א-forms can reach Avogadro's number (610^{23}). Falling אγ flows can spread through the silica of the lithosphere and condense into metabolic quanta on the night side of Earth in water-protein systems of plants and animals. The decay of ν_e is similar to the process of melting an ice cube in warm water, and in the framework of quantum physics it is modeled by mechanism of evaporation and conversion of the mass of a particle in a gravitational well. [Medvedev, 2010; Phillips, 2014].

The density and chirality of אγ flows falling on the Earth are determined mainly by physics of Sun, evolution of which from the beginning of Solar System is modulated by planetary and galactic factors. The frequencies of these modulations could manifest themselves in the geochronologies of biosphere and climate. To identify these correlations, a comparative analysis of the data from the

paleoarchive and astronomical observations was carried out, taking into account the probable mechanisms of causal relationships between physical factors and the biosphere.

2. Materials and methods

The known data of space, geophysical and paleontological observations and studies were used in a comparative analysis of influence of planetary and galactic factors on the biosphere, as well as to identify correlations between the chronologies of:

- biodiversity of marine biota and global temperature (T_G) in the Phanerozoic (Fig. 1);

- biological and geochemical disturbances, T_G and sea oxygen saturation during the global Permian-Triassic (P-Tr) extinction event ~280-240 Ma (Fig. 2);

- average annual temperatures of the surface atmosphere over the last millennium and at present from 1961 to 1990 (Fig. 3).

- the number of sunspots in the averaged Schwabe cycle (Fig. 5).

- Jupiter's effects on Solar activity (SA) in the 23rd and 24th Schwabe cycles and its orbital motion (Fig. 6).

- orientations of the magnetic dipoles of Jupiter and the Sun in the Hale cycle (Fig. 7).

- global extinctions in the Phanerozoic era and the cyclicity of the Solar System's motion around the center of the Galaxy (Fig. 8, Fig. 9).

- dynamics of sapientation and reproduction of humanity over 10 kyr (Fig. 10).

Estimates of the rates of change of physical, chemical and biological parameters of events on linear sections of chronologies were obtained from approximations by the Kt function, where K is a coefficient with the dimension [parameter/year], t is the time of change of the parameter in years. The rate constants were designated: k for changes in T and T_G, k_N for the number of marine genera. The level of reliability of the paleontological data in Fig. 1 and Fig. 2 limited the calculations of the K values to qualitative estimates. The graphical data were digitized using Adobe Photoshop, and linear approximations of the chronologies were obtained using Excel.

3. Results and discussions

3.1. Effects of chiral factor in biosystems

The standard physics of observed solar and cosmic neutrinos is limited to the statistics of individual elastic collisions of high-energy neutrinos with electrons of the active medium [Borexino, 2018; Athar, 2022]. To understand the physics of א-forms and the biophysics of אγ, it is necessary to study the synergism of chirality, temperature and nuclear spins in the mechanisms of self-organization of water-protein systems *in vitro* and *in vivo* [Avdeeva, 2016; Brookes, 2017; Knapp, 2022; Tverdislov, 2022; Naaman, 2022]. During biogenesis, a mechanism of אγ condensation in cooperative water-protein systems, including clusters of a network of fluctuating hydrogen bonds

(HBs), hydration shells of protein alpha helices, and metabolites with chiral fragments and nuclear spins, apparently evolved. ℵγ condensation is facilitated by dynamic phase transitions in tetrahedral HBs networks at 4, 25, and 37 °C [Eisenberg, 2007; Shimkevich, 2011; Liu, 2015; Kholmanskiy, 2021; 2023; Knapp, 2022; Bulavin, 2023]. Mathematical modeling of coupled systems confirms an increase in the probability and distances of quantum walks along chiral chains [Li, 2020; Annoni, 2024]. The activation energies (E_A) of the dependences of the chirality of aqueous solutions of sugars, proteins and other biomolecules on T in the range of ~0-42 °C have values from 0.1 to 0.6 kJ/mol and are close to the E_A values of cluster rearrangements in tetrahedral HBs network and transitions between nuclear ortho and para isomers of water [Zaitseva, 2016; Kholmanskiy, 2021; 2023].

Condensation of ℵγ on chiral active centers catalyzes the process of biochemical utilization of thermal energy of the environment by microorganisms, thereby regulating its T. The exothermic effect of ordering the tetrahedral structure of HBs ocean water at a high ℵγ flux density could have contributed to the emergence of the biosphere in the Archean [Dvornyk, 2003; Kholmanskiy, 2023; Shaviv, 2008; Nandy, 2021]. In subsequent eras, the imbalance between the utilization of thermal energy by the biosphere and its radiation by the oceans could have played the role of a trigger for the launch of the greenhouse effect or global cooling (Fig. 1, Fig. 2). The degree of participation of the ℵγ flux in such a mechanism of climate regulation is determined by the ratio of the sizes of the oceans and land, as well as the configuration of the continents. This partly explains the correlations of global events in the biosphere with the geochronologies of the formation and breakup of the supercontinents Rodinia (~1100-750 Ma), Pannoti (600-540 Ma) and Pangea (after ~250 Ma) [Dobretsov, 2008; Sorokhtin, 2010]. Changes in the intensity of ℵγ fluxes during periods of global events in the biosphere may also be responsible for the imbalance between the natural distribution of carbon, sulfur, and oxygen isotopes (Fig. 1, Fig. 2).

It is known [Avdeeva, 2016; Brookes, 2017] that enrichment of a biosystem with isotopes of elements having a nuclear spin leads to acceleration of enzymatic and other biochemical reactions. Possible interaction of ℵγ with magnetic moments of such isotopes will lead to orientational correlation of spins in chemically active centers, enhancing the magnetic effect in reactions involving ion-radical pairs [Brookes, 2017]. ℵγ will have the greatest influence on the kinetics of enzymatic proton transfer in transmembrane ion and water channels, as well as in reactions limiting the biochemistry of circadian rhythms, mitosis and mutagenesis [Michel, 2007; Brookes, 2017; Bloom, 2017; Mishra, 2020; Naaman, 2022]. The mechanisms of action on the biosphere of ℵγ flows emanating from the earth at night will differ significantly from their action during the day, both due to the absence of sunlight and a decrease in temperature at night [Kholmanskiy, 2019]. These differences apparently determined the genesis of the circadian clock of the biosphere and the mechanism of switching the neurophysiology of animals from the wakefulness mode to the sleep

mode [Michel, 2007; Kholmanskiy, 2019; Dvornyk, 2003]. The increased density of אγ fluxes in the lithosphere faults may well accelerate evolution and differentiate the genesis of new animal species through mutagenesis of chiral protein complexes in their genomes [Goodman, 1990; Markov, 2009]. The combination of the effect of אγ on biosystems and radiation of terrestrial radioactive elements, including antineutrinos from beta decay, could ensure the genesis of bilateral organisms in the Ediacaran period and the visual system in animals during the Cambrian explosion [Lupovitch, 2004; Baguñà, 2008; Langmuir, 2012; Zhang, 2013; 2014; Kataoka, 2014; Isozaki, 2014; Daley, 2019]. It is believed [Matyushin, 1986; Kholmanskiy, 2020] that in the uranium provinces of the Great African Rift Valley during the Paleolithic era (~3 Ma), under the influence of אγ and argon-222 radiation [Beckman, 2024], the homo habilis genome mutated into the homo sapiens genome, in which 800-700 thousand years ago a gene responsible for the development of speech ability appeared and this accelerated the process of sapientation [Enard, 2002; Markov, 2009; Kholmanskiy, 2012].

3.2. Geochronology of global events in biosphere

Estimates of the reproduction rates of marine biota during the Cambrian ("Cm"), Ordovician ("Or") and during the Mesozoic-Cenozoic ("Md") are shown in the boxes in Fig. 1. The k_N values for the "Cm" and "Md" faunas were close and three times smaller than the k_N for the "Or" fauna (Fig. 1A). The k_N estimate for "Or" was made without taking into account the "Cm" fauna, which became extinct by the end of the Paleozoic "Pz" [Sepkoski, 1984; Rohde, 2005]. When estimating the k_N of the "Md" fauna, the surviving "Pz" fauna was taken into account [Sepkoski, 2002]. Judging from the graphs in Fig. 1 and Fig. 2A, the global extinctions of marine faunas Ordovician-Silurian (Or-S), Permian-Triassic (P-Tr) and Cretaceous-Paleogene (Cr-Pl) lasted ~5 Myr. It follows that the rates of global extinctions were 3-4 orders of magnitude higher than the rate of growth of species and numbers of animals in the periods "Cm", "Or" and "Md" (Fig. 1).

Figure 2 shows the geochronologies of changes in biosphere parameters during the P-Tr event with a relatively high time resolution. A comparison of the k values of T_G and T changes at sea surface shows that the slow increase in T_G correlates with the synchronous cooling of hydrosphere. When the P-Tr event mechanism is triggered, the k moduli of T_G and T changes, as well as the rate of seawater deoxygenation, increase by almost an order of magnitude. At the same time, the [^{34}S] and [CO_2] content increased and [^{13}C] disturbances intensified (Fig. 2). The difference in the triggering mechanisms and causes of extinction in Or-S and P-Tr is indicated by different directions of T_G jumps at points of ~450 Ma and ~250 Ma against the background of the averaged T_G, the value of which fluctuates with a period of ~150±20 Myr throughout the Ediacaran and Phanerozoic (Fig. 1B).

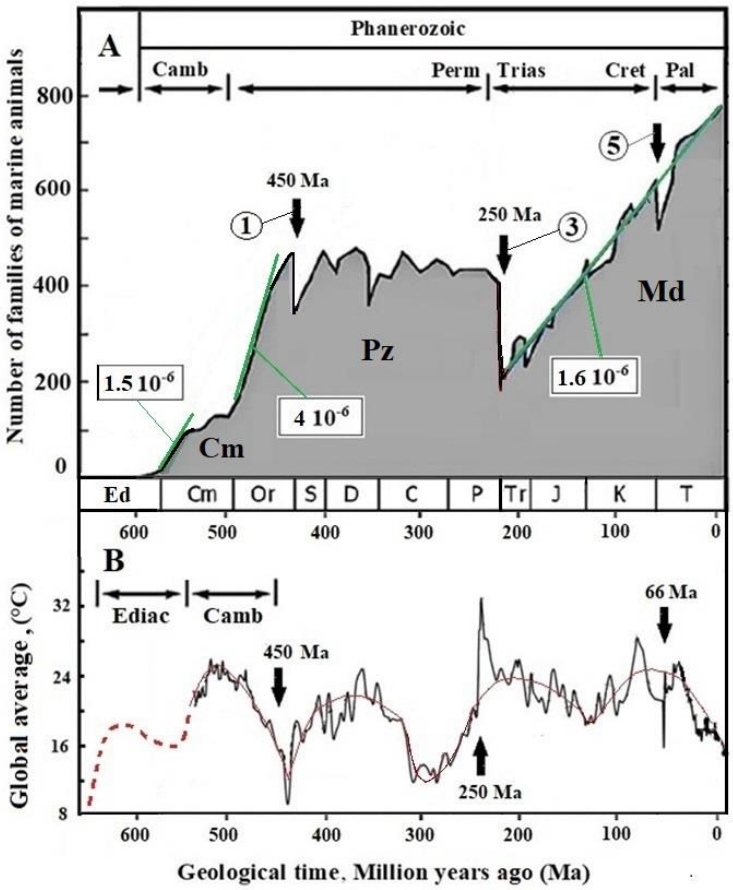

Fig. 1. Geochronologies of the number of marine animal families (**A**) and global temperature (**B**). Pz – Paleozoic, Md – Mesozoic-Cenozoic, Ed – Ediacaran, Cm – Cambrian, Or – Ordovician, S – Silurian, D – Devonian, C – Carboniferous, P – Permian, Tr – Triassic, J – Jurassic, K – Cretaceous, T – Tertiary, Cz – Cenozoic. Arrows mark the onset of global extinctions: (1) Ordovician-Silurian (~450 Ma), (3) Permian-Triassic (~250 Ma), and (5) Cretaceous-Paleogene (~66 Ma). Green and red lines in **A** are approximations ($k_N t$) of family growth and extinction, boxes show k_N values ($Year^{-1}$). In **B**, the red line is the average envelope, the dotted line is the probable course of T_G in the Ediacaran. The original N and T_G dependencies are adapted from [Sepkoski, 1984; Sepkoski, 2002; Rohde, 2005; Scotese, 2021].

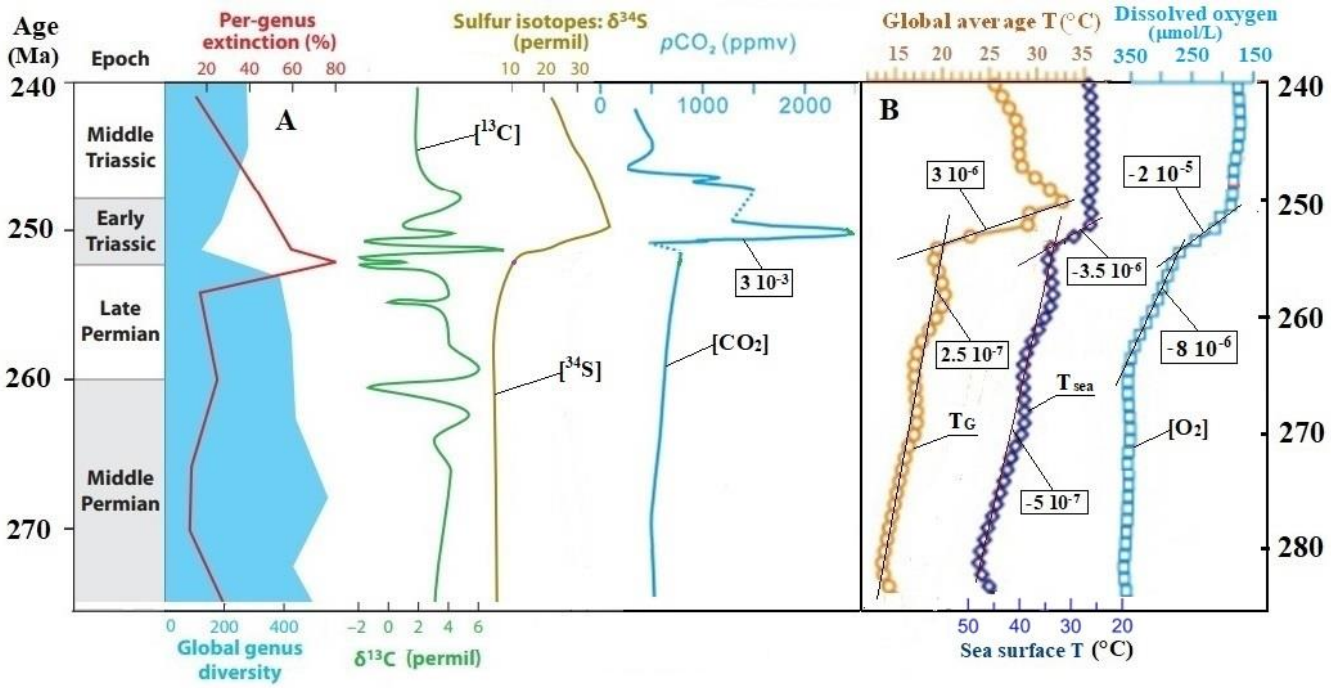

Fig. 2. Geochronologies during the Permian-Triassic event. **A**, biological and geochemical perturbations of [^{13}C], [^{34}S], and [CO_2] concentrations. **B**, global temperature (T_G), sea surface (T_{sea}), and sea oxygen saturation ([O_2], C_O = mmol/L) temperatures (°C). Lines in **B** are Kt approximations of the T_G, T_{sea}, and [O_2] geochronologies, with boxes showing K values in °C/Year and C_O/Year. Figures **A** and **B** are adapted from [Payne, 2012] and [Song, 2023], respectively.

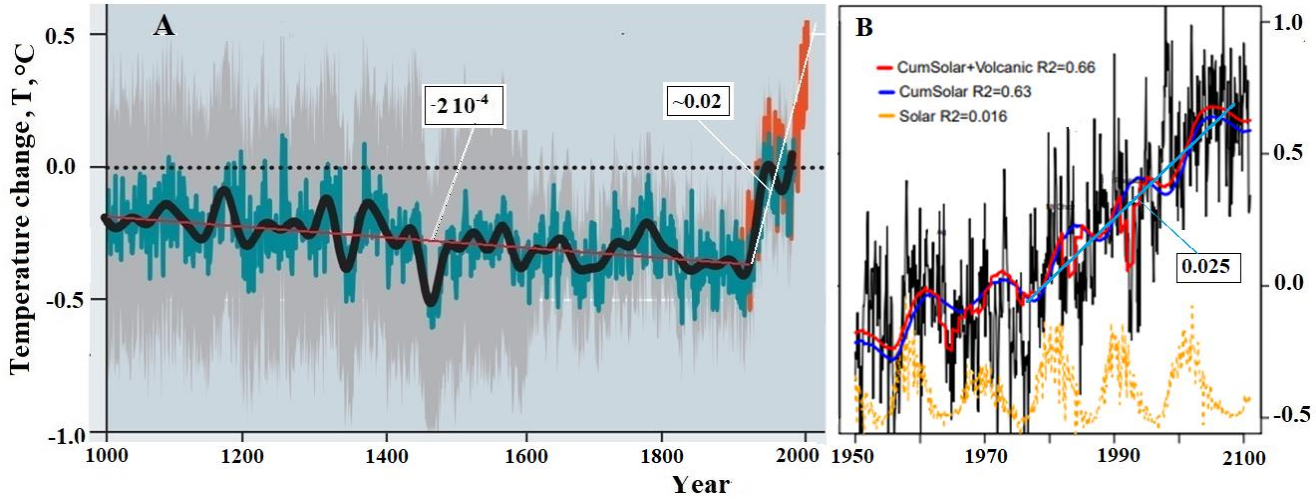

Fig. 3. A. Timeline of deviations of average annual surface atmospheric temperatures T °C per thousand years from the average annual value calculated for the period from 1961 to 1990. **B**. Cumulative solar irradiance (blue) and volcanic forcing (red) is highly correlated with land surface global T (black). The direct solar irradiance (orange). The boxes contain the values of k [°C/Year] of the linear approximations (kt). Figures **A** adapted from [Mann, 1999], **B** from [Scafetta, 2023].

The k_N estimate for rate of decline in the number of marine families in Paleozoic 100 Myr years before the onset of the mass extinction in the P-Tr event is -0.7 Myr^{-1} and almost coincides with the k estimate for the decline in sea surface temperature at the end of the Permian, equal to -5 10^{-7} °C/Year (Fig. 2B). The decline in sea temperature and oxygen concentration in seawater during the mass extinction period accelerates by 7 and 2.5 times, reaching, respectively, values of -3.5 10^{-6} °C/Year and -2 10^{-5} mM/Year (Fig. 2B). Such changes in the living conditions of marine animals apparently lead to their mass extinction.

The emergence of life on Earth was predetermined already at the stage of formation of the Solar system (SS). Due to the unique physics of planet Earth and its position in the SS, a stable hydrosphere was formed and a synthesis of heterochiral biosystems capable of evolution was realized. With an average annual temperature on the Earth's surface of ~7 °C, on neighboring planets Venus and Mars it was ~460 °C and -65 °C, respectively, and they did not have liquid water, which occupies ~70% of the surface on Earth [Sorokhtin, 2010]. The geochronology of the biosphere is replete with global events characterized by blurred dating and ambiguity of models of participation of cosmic and terrestrial factors in them [Dobretsov, 2008; Scotese, 2021; Palin, 2020; Planavsky, 2021]. The entire complex of these factors ensured the regulation and maintenance of the T_G of the Earth's hydrosphere over long periods of geochronology in the range of ~0-42 °C, in which the thermodynamics of hydrogen bonds of water (HBs) maintains the viability of water-protein systems.

During the Catercheian era (~4570-4000 Ma), the formation of the Earth's structure with the formation of the lithosphere was completed. The thermal regime of the biosphere began to depend to a greater extent on solar radiation [Pittock, 2009], the luminosity of which, with an increase of ~6% per billion years by the end of the Archean (~2500 Ma), remained weak [Bahcall, 1982; Nandy, 2021]. Under these conditions, the occurrence of global glaciation of the Earth was prevented by thermophysical effects in the atmosphere, the nitrogen-saturated crust of the continents [Goldblatt, 2009]. In the warm and humid climate of the Archean, anaerobic biosynthesis ensured the development of a biota of unicellular microorganisms with organic membranes [Fedonkin, 2003; Butterfield, 2007; Langmuir, 2012]. At the end of the Paleoproterozoic (~1600 Ma), stellar dynamics in the Galaxy and planetary dynamics in the Solar System reached a stationary regime and the luminosity of the Sun increased relative to the Caterpillar by 27% [Bahcall, 1982; Pittock, 2009; Zhang, 2017]. Under these conditions, the geophysics and climate of the Earth ensured the formation of the first supercontinent from the lithosphere plates [Sorokhtin, 2010; Spencer, 2018] and the appearance of photosynthetic cyanobacteria, which saturated the atmosphere and hydrosphere with oxygen [Bachan, 2015; Eguchi, 2019; Lyons, 2014; Boag, 2018]. An increase in the proportion of ^{12}C in the products of photosynthesis and a decrease in the proportion of ^{13}C in organic carbon led to an increase in $\delta^{13}C$ in CO_2 and in the bottom layers of the Proterozoic hydrosphere (Lomagundi event). Later, the geochronology of climate and global events began to be modulated to varying degrees by cosmic factors of three levels – solar, planetary and galactic. During the Ediacaran period (~635-540 Ma), the entire complex of geophysical and cosmic factors ensured the formation of conditions in the hydrosphere necessary for the evolutionary explosion of biodiversity in the Cambrian ~540-485 Ma. According to geochronology, the “Cambrian explosion” was preceded by abnormally high velocities of lithospheric plate movement. The transformations of the lithosphere were apparently accompanied by the formation of near-surface silica layers in it, which played the role of waveguides for אγ. An increase in the intensity of אγ flows emanating from the lithosphere could have initiated the emergence and development of spiral and bilaterally symmetrical (bilateria) forms of multicellular organisms in an aquatic environment enriched with calcite in the Precambrian.

A significant role in the kinetics of biosynthesis is played by local T and global temperature (T_G) [Song, 2023], the geochronology of which clearly correlates with some global events in the Proterozoic and Phanerozoic (Fig. 1 and Fig. 2). The duration of each of the five bell-shaped curves of T_G changes in the Ediacaran and Phanerozoic ~130±20 Myr (Fig. 1B) is comparable with the characteristic time of the periods of macroevolution and is one or two orders of magnitude greater than the duration of molecular and morphological changes at the stages of microevolution [Rolland, 2023]. These stages are associated with periods of ~10 Myr of a sharp decrease in T_G during the Or-S mass extinction (~450 Ma, Fig. 1B) and a jump in T_G during P-Tr (250 Ma, Fig. 1, Fig. 2B) [Fan,

2020; Wang, 2019; Edwards, 2015; Burgess, 2014; Sun, 2012; Song, 2023]. The proximity of the growth rates of marine biota at the beginning of Phanerozoic (3.5 10^{-6} $Year^{-1}$) and after the P-Tr extinction (3.0 10^{-6} $Year^{-1}$, Fig. 1) indicates the relationship of the abiogenic factors of macroevolution active during these periods [Harmon, 2021; Rolland, 2023]. The Cretaceous-Paleogene extinction of dinosaurs in the vicinity of 65 Ma is explained by the darkening of the atmosphere by emissions of substances during the fall of a large asteroid and the activation of volcanism. The sharp decline in T_G due to solar radiation shielding and atmospheric poisoning with toxic gases and aerosols probably led to the extinction of certain animal species, including dinosaurs. It should be noted that the mass P-Tr and Cr-Pl extinctions (Fig. 1) could have contributed to selection and reproduction in the order of mammals of the hominid family of primates [Osozawa, 2023].

The dynamics of continental plate tectonics after the Archean, affecting the water/land ratio and water chemistry, initiates global changes in T_G and climate, which lead to explosive growth or reduction of biodiversity in marine biota [Song, 2019; Smith, 2007]. Perturbations in the neutrino physics of the Sun and solar-terrestrial connections caused by planetary and galactic factors can contribute to the mechanisms of triggering global events in geophysics and the biosphere.

3.3. Jupiter and heliophysics of Earth's climate

From the Archean to the present day, the main factor in the ecology of biota and the sapientation of homo has been and is the synergy of heliogeophysics, modulated by the dynamics of the planetary system for the last ~250 Myr [Langmuir, 2012]. Due to gravity and interactions of magnetic dipoles, the Sun and planets of Solar System (SS) are in dynamic equilibrium and rotation of planets around Sun, in first approximation, obeys Kepler's third law:

$$R^3 \sim P^2, \qquad (1)$$

R is the distance between the centers of mass of the planet and the Sun, *P* is the period of the orbital rotation of the planet. Due to bulk and heterogeneity of matter of planets and Sun, gravitational forces can cause tidal effects on Sun, the magnitudes of which directly depend on their masses and are inversely proportional to R^3. The magnetic effects of planets on Sun are determined by a similar dependence on R^3 and on the magnitudes and mutual orientation of their magnetic dipoles (μ).

Table 1. Magnitudes of planetary tides and magnetic effects on Sun relative to Earth

Sun, Planet	P (yer)	Mass	μ [Magnetic]	R (AU)	Tides	Magnetic
Sun	-	3.3 10^5	4.4 10^6	0	-	-
Mercury	0.24	0.06	4.7 10^{-4}	0.31-0.47	0.55-1.85	7 10^{-3}
Venus (V)	0.62	0.82	1.0 10^{-5}	0.72	2.2	2.7 10^{-5}
Earth (E)	1	1	1	1	1	1
Mars	1.88	0.11	2.6 10^{-5}	1.52	0.03	7 10^{-6}
Jupiter (J)	11.86	318	1.9 10^4	4.95-5.46	2.0-2.7	140
Saturn	164.8	95	576	9.54	0.11	0.66

Taking the tabular values of these parameters and Earth's effects as a unit, we estimated the relative values of tidal and magnetic effects for the SS planets (Table 1). It follows from Table 1 that the leading gravitational and magnetic "gear" of the heliophysical clockwork is Jupiter. The tidal component of this mechanism sums up the effects of Jupiter (J), Venus (V) and Earth (E) and reaches a maximum when the planets J, E and V are aligned on a line passing through the Sun on one or both sides of it (syzygy). The frequency of JEV syzygies determines the 11-year cyclicity of Solar activity (SA) manifestations through changes in the number of sunspots (Wolf numbers, W), as well as the intensity of 10.7 cm radio waves and flares [54, 103, 104, 105]. Mercury does not fit into these syzygies and does not participate in the maximum tidal effect on Sun [Okhlopkov, 2020]. From the calibrated chronology of W in both hemispheres of Sun from 1876 to 2020 [Manda, 2020; Hathaway, 2010], the average duration of the Schwabe cycle T_S = 10.8 ± 5% of the year follows. Two adjacent Schwabe cycles are combined into one Hale magnetic cycle (~22 years), during which polarity reversal of fields of northern and southern halves and global field of Sun occurs [Hathaway, 2010; Okhlopkov, 2020; Livshits, 2006; Pipin, 2006; Leamon, 2022]. Calculations of T_S taking into account the frequency of JEV- syzygies and JEV+Saturn syzygies [Space] on the magnetohydrodynamics of the convective zone of the Sun give values 11 and 22 years, close to the measured T_S, but less than the orbital period of Jupiter P_J = 11.86 years [Nandy, 2021; Hathaway, 2010; Vita-Finzi, 2022; Okhlopkov, 2020; Cionco, 2023; Fan, 2021; Stefani, 2019]. Since the eccentricity of J is 3 and 7 times greater than that of Earth and Venus, the effect of J in the vicinity of perihelion will be $(5.46/4.95)^3$ ~ 1.35 times greater than at aphelion, while for V and E this difference is insignificant. Because of the inclination of the plane of J's orbit by 1.3°, its perihelion will be located below the ecliptic, and the tidal and magnetic effects of J on the southern and northern halves of Sun will differ.

The helioseismological data made it possible to deepen the kinematics of the dynamo models of the SA “tachometer” to level of tachocline [Stefani, 2024; Charbonneau, 2022; Seker, 2013] and core of Sun [Grandpierre, 2005; Nataf, 2022], which rotates significantly faster than matter of radiative zone [Fossat, 2017]. Within the framework of the dynamo models of convective zone, the mechanisms of generation and reversible circulation from equator to poles of pairs of differently directed poloidal magnetic fields generated by ring and differently directed large-scale currents in tachocline (Fig. 4A, Fig. 4B) are calculated [Muñoz-Jaramillo, 2009; 2010; Nandy, 2021; Hotta, 2021]. At the same time, question of mechanisms of activation of currents and “tachometer” itself remains open; there is also no clear answer about the role of tidal effects of planets in cyclization of dynamics of sunspots and, even more so, in reversal of Sun’s magnetic field [Hathaway, 2010; Okhlopkov, 2020; Nataf, 2023].

An indirect confirmation of tidal effects of Jupiter and Venus on the Sun (Table 1) can be their influence on orbital motion of Earth. In works [Wilson, 2013; Kent, 2018; Hinnov, 2018]. Comparison of the results of astronomical analysis and paleoarchive data on climate and geochemistry geochronologies up to ~50 Ma made it possible to reveal a cyclicity with a period of ~405 kyr. Numerical integration of high-precision ephemerides showed that this cycle is associated with rhythm of precession and eccentricity of Earth's orbit [Laskar, 2011]. These changes, according to Milankovitch, cause fluctuations in insolation of Earth's surface and synchronous climate changes. This mechanism could contribute to the development of global events in the biosphere after the P-Tr mass extinction.

The magnetic effect of Jupiter on the Sun (J_μ effect) dominates, since the influence of the Earth and Saturn does not exceed ~1% (Table 1). In this case, the J_μ effects of Jupiter at perihelion and aphelion differ by a factor of 1.35. This difference changes continuously as J moves along its orbit, since the interaction energy (M) between the magnetic dipoles of Sun (μ_S) and Jupiter (μ_J) depends on angle between them (f_{SJ}), as well as on the angles between the dipoles and the rotation axes of Sun and J (f_S and f_J):

$$M \sim \mu_S \, \mu_J \, \frac{cos f_{SJ} - 3 cos f_S \, cos f_J}{R^3} \qquad (2)$$

The values of f_S and f_J are equal to 7.25° and -9.6° (Fig. 4) and the maximum value of f_{SJ} taking into account angle of inclination of J axis of 3.3° and plane of J orbit (1.3°) to plane of ecliptic will be ~21.5°. The dependence of the value of f_{SJ} on rotation of Sun and J around their axes can cause modulation of J_μ effect by frequencies equal to the rotation periods of the Sun (~27 days) and J (~10 hours). Global ring currents in the vicinity of the tachocline of the Sun and in the surface layers of Jupiter [Hori, 2023] (Fig. 4A, Fig. 4C), like alternating windings of inductive coils, can generate magnetic dipoles and quadrupoles (Fig. 4B) [Livshits, 2006]. If the values of ratios μ_S/μ_J ~230, radius of the tachocline (~0.7 of radius of Sun [Horstmann, 2023]) and current sheets of Jupiter (~0.9 of the radius J, Fig. 4D) are substituted into formula $\mu = \pi I r^2$, we obtain ratio of values of ring currents I_S/I_J ~ 4, which conditionally correlates with four current rings of the Sun and one ring of J. The interaction between dipoles and the resonant transfer of energy between ring large-scale currents according to the scaling law [Glattfelder, 2018] can be carried out in the same way as between Tesla coils [Singh, 2012].

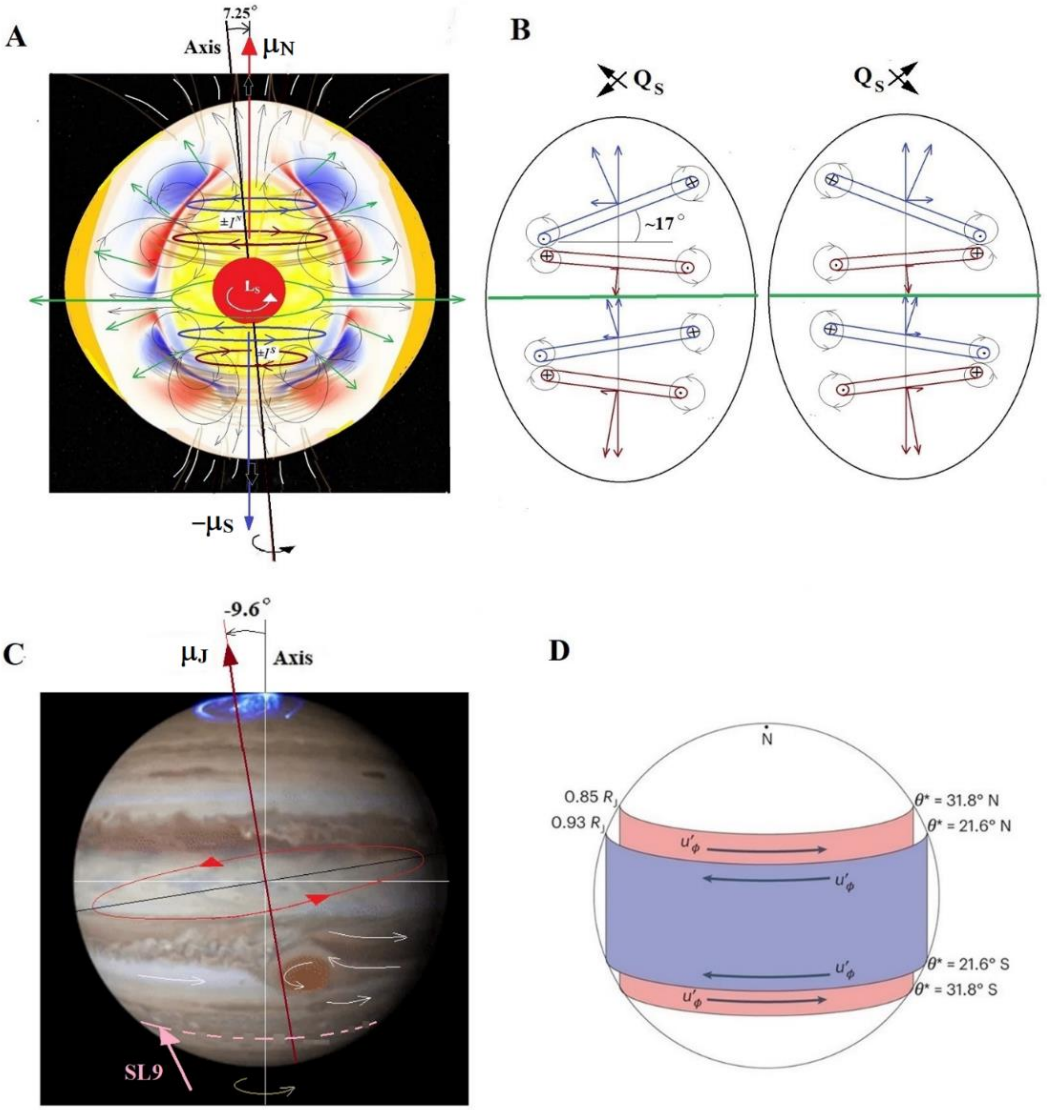

Fig. 4. A – model of distribution of ring currents (black and red circles), radial magnetic field (green arrows) and poloidal magnetic fields (circles around red and black zones above tachocline) in convective zone of Sun (yellow color), μn and –μs magnetic dipoles of the northern and southern hemispheres of the Sun. **B** – schemes of configurations of ring currents of Sun, responsible for quadrupole magnetic moments (Q_S). **C** – photo of Jupiter, μ_J – magnetic dipole of the ring current of Jupiter (red circle), white arrows – atmospheric flows in the vicinity of the Red Spot, pink arrow and dotted curve – trajectory of falls of 21 fragments of comet Shoemaker-Levy (SL9). **D** – scheme of distribution of current sheets of Jupiter. **A** is adapted from [Nandy, 2021; Stefani, 2019; Hathaway, 2010], **B** from [Gavelya, 2018] and D from [Hori, 2023].

In Fig. 5A shows the averaged Schwabe cycle from [Hathaway, 2010] and physically adequate approximations of the ascending and descending branches by third-degree polynomials. Their reliability is not inferior to abstract functional F(t), which is used in [Hathaway, 2010] for ideal approximation of the Schwabe cycle by selecting four arbitrary parameters and Gaussian exponent:

$$F(t) = A\left(\frac{t-t_0}{b}\right)^3\left[\exp\left(\frac{t-t_0}{b}\right)^2 - c\right]^{-1}$$

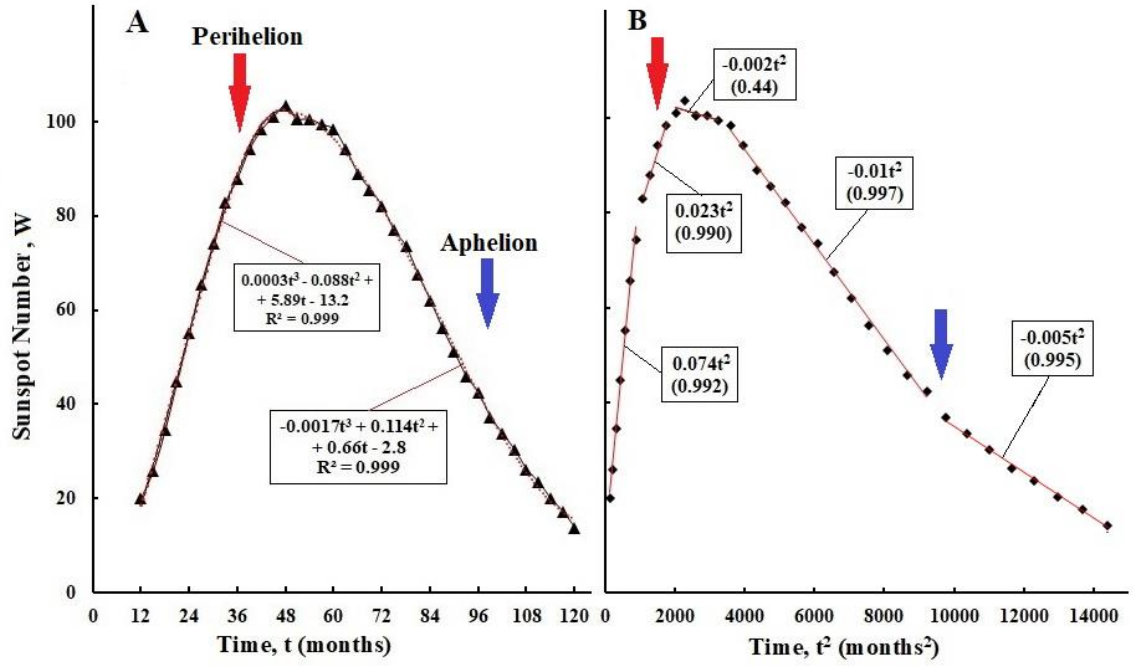

Fig. 5. A – approximations by third-degree polynomials of the averaged Schwabe cycle from [Hathaway, 2010], B – physically adequate approximations of the ascending and descending branches of the Schwabe cycle (see text). Red and blue arrows – perihelion and aphelion of Jupiter's orbit.

To identify the contribution of the J_μ effect to the chronology of cycles, Schwabe and Hale used physically adequate functions to approximate the Schwabe cycle. Due to the dependence of the tidal and magnetic effects on R^3, their total or separate contribution according to (1) should depend linearly on the square of the current time of the J-orbit (t^2). Indeed, the ascending and descending branches of the Schwabe cycle are divided into two intervals, the kinetics of which are approximated by the $C_N t^2$ functions with different slopes (C_N). For ~2 years after J passes the perihelion and aphelion points (red and white curves in Fig. 6B), the W values differ little from the maximum and minimum values, respectively (Fig. 5, Fig. 6A). On the red segment of the J orbit, apparently due to resonant interactions between the dipoles of the Sun and Jupiter, the inclination angles of the planes of the ring currents of the J orbit and the Sun change, as a result of which the resulting dipole μ_S is transformed into a quadrupole QS (Fig. 4B, Fig. 6A). Disturbances of the magnetic fields of the tachocline ring currents twist the radial currents of the convective zone into spirals at latitudes from 15° to 55° in both hemispheres, generating sunspot magnetic fields of a poloidal configuration [Hotta, 2021; Havelaya, 2018]. On the white segment of J orbit, when J_μ effect weakens and its sign changes, relaxation of large-scale currents on Sun occurs and their total magnetic dipole changes sign ($-\mu_S$).

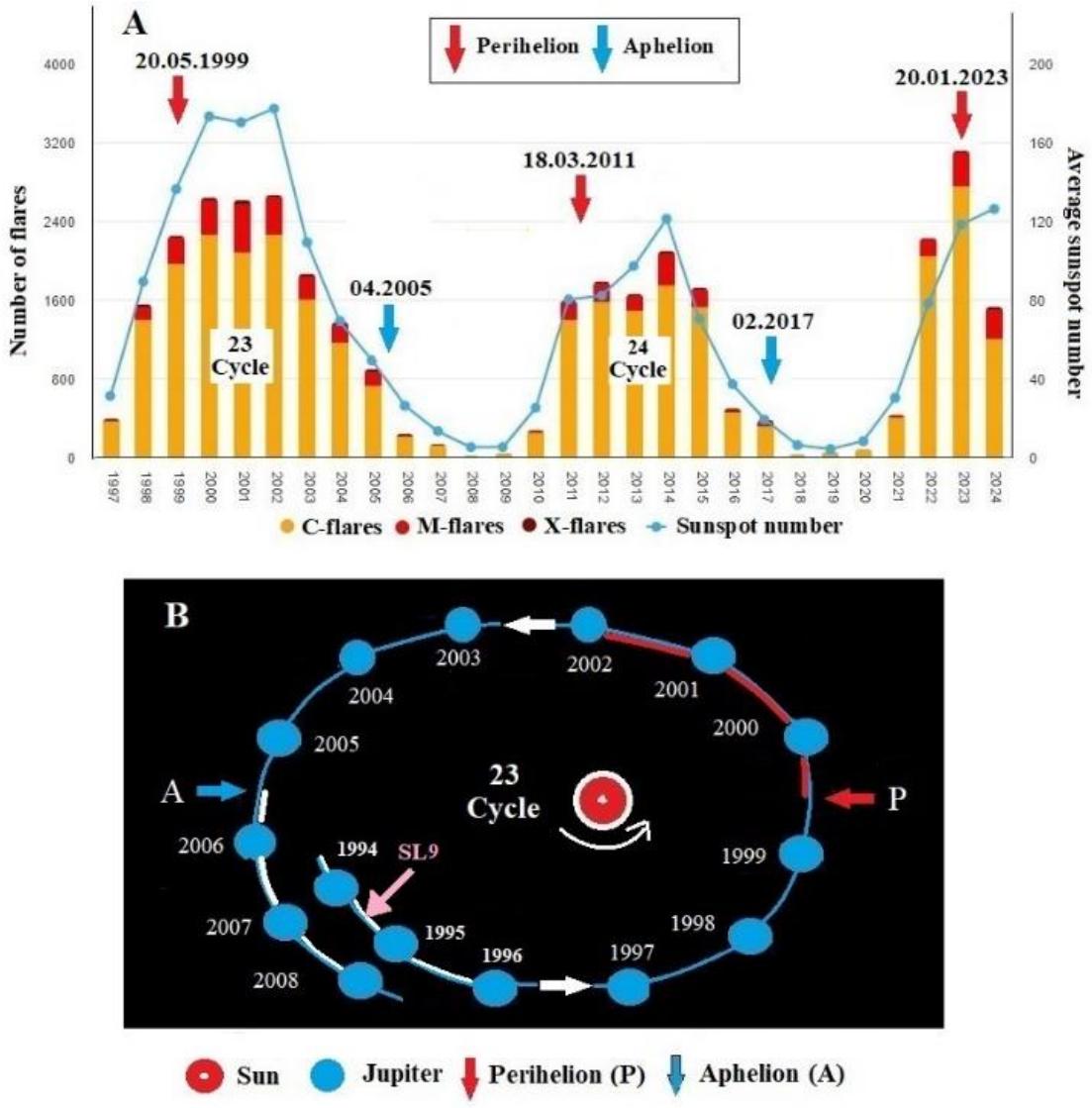

Fig. 6. A – chronology of changes in the number of flares and spots in the 23rd and 24th SA cycles, red and blue arrows – the time of Jupiter's position at perihelion and aphelion. **B** – diagram of Jupiter's orbit during the 23rd SA cycle, pink arrow – the moment of the Shoemaker-Levy (SL9) falls onto Jupiter. Original data from [Jupiters; Space].

The fall of comet Shoemaker-Levy 9 (SL9) occurred in 1994, when Jupiter was at aphelion, and the Sun, accordingly, at the SA minimum (Fig. 6A, Fig. 6B). According to estimates, the fall of SL9 released energy equivalent to several million megatons of TNT (which is 600 times greater than the world's nuclear arsenal) [Impact]. 21 fragments of the comet crashed into the southern hemisphere of Jupiter at a latitude of ~44° with an interval of ~7 hours with a rotation time of J around its axis of ~10 hours [Impact]. Apparently, at a latitude of ~44° a necklace of plasma clots of ionized elements was formed, the electrodynamics of which, through disturbances of nearby current rings of southern hemisphere J, caused changes in its magnetic field J. Since traces of the explosions remained on the surface of J for more than a year, it can be assumed that during the relaxation of the axisymmetric currents of the southern hemisphere, a new value of μ_J was recorded and, accordingly, the J_μ effect decreased. These effects of SL9 on the resonant interaction of μ_S and μ_J led not only to a significant

decrease and distortion of the course of SA 23 and 24 cycles (Fig. 6A) [Toma, 2009; Sheeley, 2009; Vidotto, 2018], but also manifested themselves in geomagnetism [Zerbo, 2013; Hady, 2013; Hady, 2009].

Thus, the SA mechanisms and the μ_S reversal during the Hale cycle (Fig. 7A) integrate all the factors of the dependence of the J_μ effect on the distance and orientation of μ_J relative to Sun. These disturbances of the physics of Sun over 2 years apparently lead to a decrease in the intensity of the ℵγ fluxes, which causes a decrease in the efficiency of thermal energy utilization by the biosphere and explains the two-year periods of increasing global T_G on Earth. These factors are not characteristic of tidal effects, and the ranges of changes in J_μ effect clearly illustrate the electromagnetic connections of "hot Jupiter" with its star [Cauley, 2019] and Jupiter with Io [Schneider, 2007].

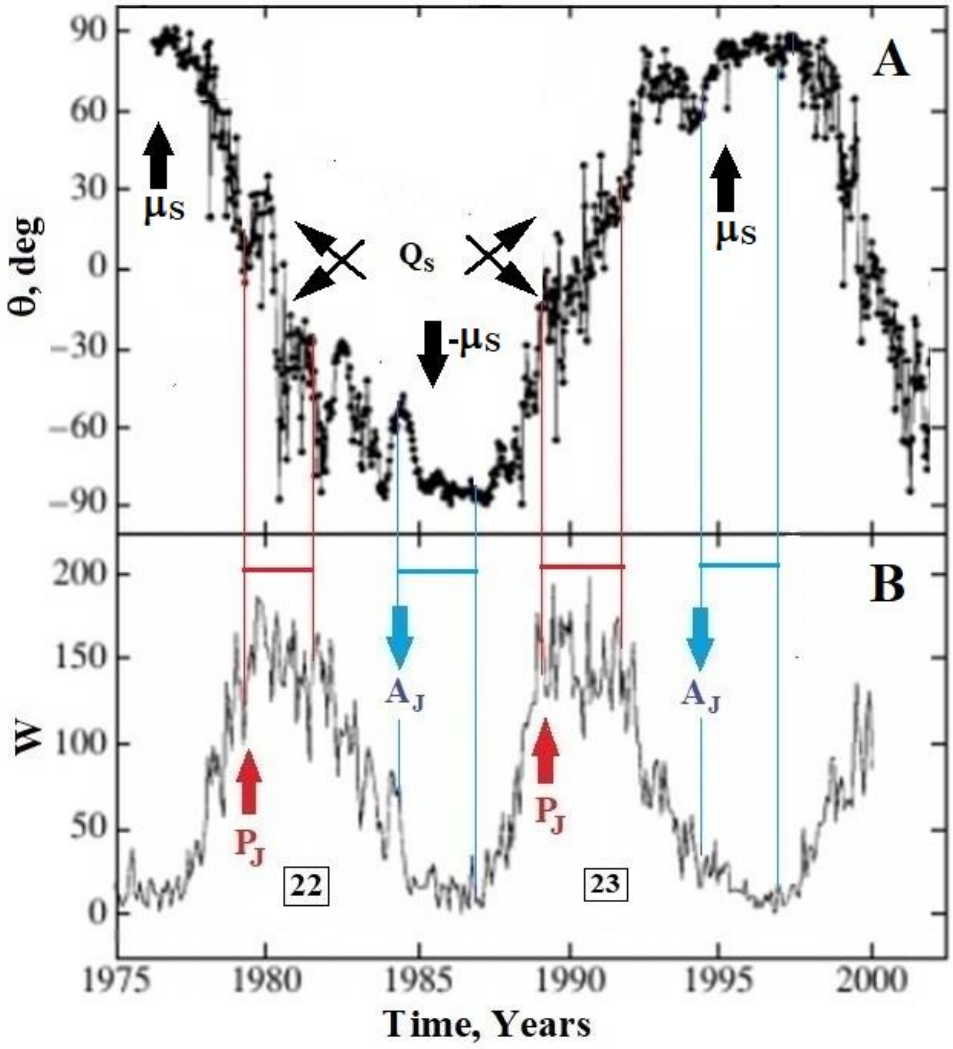

Fig. 7. A – chronology of the change in the angle of the Sun's dipole (θ) during the reversal of its magnetic field in the Hale cycle during the 22nd and 23rd SA cycles. **B** – correlation of 22nd and 23rd Schwabe cycles with position of Jupiter at perihelion (P_J) and aphelion (A_J), red and blue arrows. The figure is adapted from [Livshits, 2006].

When constructing hypothetical models of Sun and Jupiter, one should take into account the universality of the scaling law [Glattfelder, 2019]. It is based on the universal laws of dialectics and quantum rules of self-assembly of chiral elements of elementary particles and nuclei from dichotomous energoforms similar to א-forms of neutrinos [Kholmanskiy, 2017; 2019]. Self-assembly-condensation of energoforms according to the bootstrap mechanism is quantized not only by Planck's constant, but also by the Avogadro number, which limits the values of the similarity coefficients between the energy and spatio-temporal parameters of the levels of the world hierarchy [Kholmanskiy, 2019; 2020]. The ratios between the radii of the helium nucleus (~1.2 10^{-13} cm) and the Sun (~7 10^{10} cm), as well as between radius of hydrogen atom and orbit of Jupiter, are close to Avogadro's number. The ratio of masses of the Sun and Jupiter is of the same order as ratio between proton and electron. The magnetic dipoles of Sun and Jupiter in Fig. 4, corresponding to ring currents, can be modeled by the quadrupole of triplet state of deuteron, in which axis of outer orbital is not coaxial with axis of shell [Kholmanskiy, 2017].

The core of Sun, like a helion, consists of a shell and two pairs of orbitals adjacent to it, inner and outer (Fig. 6B) [Vorontsov, 1981; Kholmanskiy, 2017; 2019]. In shell, thermonuclear synthesis occurs with generation of photons and neutrinos, the former are responsible for entire spectrum of electromagnetic radiation of Sun, and the latter, decaying into א-forms, form chiral photon-neutrino quanta אγ with photons of radiant zone, which have zero mass and move along the lines of force of magnetic field at speed of light [Hoyle, 1981; Bahcal, 1982; Sivaraman, 2010]. In real scale, a clear illustration of models of the helium core and the core of the Sun is electromagnetic diagram of Tokamak thermonuclear reactor project.

3.4. Galactic factors

In Fig. 8 location of highs and lows in the graph Fig. 1A was preserved after the exclusion of isolated cases and poorly dated genera in [Rohde, 2005]. Statistical analysis using Fourier and Monte Carlo methods [Rohde, 2005; Melott, 2010; 2010a; Medvedev, 2007] made it possible to approximate the geochronology of Phanerozoic marine genera by smooth sine waves with periods of 62±3 and 140 Myr, as well as by a cubic polynomial for two different regions of geochronology before and after 250 Myr. Statistically significant periods of sinusoids 62 ± 3 Myr in Fig. 9A are consistent with our estimates of the intervals in Fig. 8 between the maxima from 0 to 6 and the minima from 0* to 4*, equal to 62 ± 5 Myr. The less statistically reliable sinusoid with a period of 140 Myr [Rohde, 2005] falls into the range of periods of the T_G geochronology ~120÷140 Myr in Fig. 1B.

Note that from the array of empirical geochronologies of Phanerozoic, any macrocycle longer than ~1 Myr can be easily obtained using mathematical statistics, but it is usually not possible to establish unambiguous causes of biotic cycles using paleontology [Erlykin, 2017; Wilson, 2024; Smith, 2005; Boulila, 2021; 2023]. Moreover, a thorough astronomical and paleontological analysis

of geochronologies of biota and planetary dynamics of SS showed that up to ~50 Ma, the Earth's orbit stably changes only with a period of about ~0.4 Myr according to Milankovitch mechanism, which is associated with tidal effect of Jupiter and Venus [Laskar, 2011a].

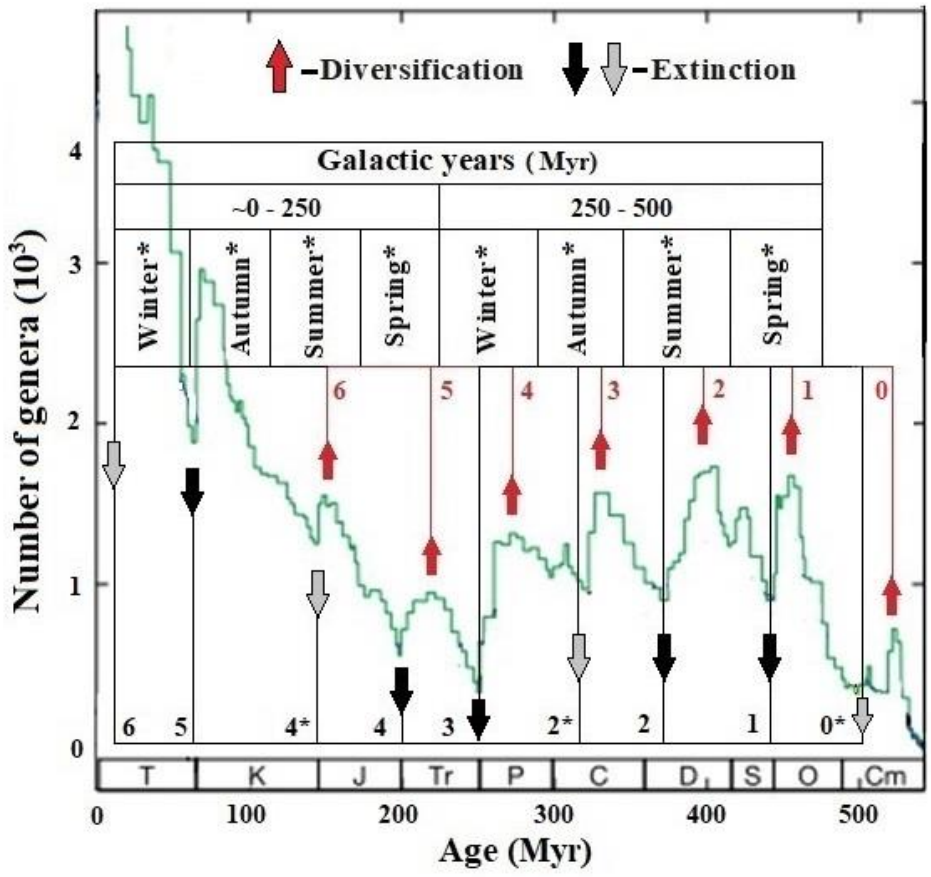

Fig. 8. Division of the geochronology of marine genera into a galactic year and four conventional seasons. Asterisks mark extinctions that are not classified as global and with fuzzy dating. Black arrows indicate extinctions, red arrows indicate maximum biodiversity. Adaptation of figures from [Rohde, 2005; Sepkoski, 2002].

It can be assumed that mechanisms of biotic cycles with periods of ~62 and ~140 Myr are associated with regular changes in gravitational potential on galactic orbit of SS. Empirical cycles in geochronology of Phanerozoic marine biota are consistent with periods of sine wave in trajectory of Sun of ~60 Myr [Klesman, 2020] (Fig. 9B) and duration of galactic year of 230-250 Myr [Leong, 2002]. The Phanerozoic era can be divided into two conventional galactic years 500-250 Myr (I-year) and 250-0 Myr (II-year) with half-years of 120-140 Myr. In this case, periods of 62 Myr between regular minima and maxima on geochronologies of marine biota will correspond to conventional four seasons of the galactic year (Fig. 8). Each season includes an interval of decline-growth of the genus population from the average value to level of global extinction, indicated by black arrow, as well as an interval of growth-decline with a maximum, indicated by red arrow in Fig. 8. These waves of extinction and reproduction of marine biota significantly differ in information amplitudes and duration from ideal Fourier sinusoid (Fig. 9A). In empirical geochronology of I-year, all four seasons

are distinguished, and in spectrum of II-year, the regular boundary between Autumn* and Winter* was blurred by the 5th global extinction at ~65 Ma, caused by an accidental fall of an asteroid.

The significant difference in geochronologies of I-year and II-year biota (Fig. 1A) is apparently due to genesis of geophysics in context of evolution of heliophysics and entire planetary system [Valentine, 1970; Sepkoski, 1997]. In I-year (~540-300 Ma), the supercontinent Pannotia was transformed into Pangea, combined with the drift of continental plates from southern to northern latitudes [Salles, 2023]. The breakup of Pangea in the II-year after ~250 Ma led to formation of the modern configuration of continents in the northern latitudes by 65 Ma. During the transformation of Pannotia into Pangea and its subsequent breakup, the area of coastal shallow water increased [Wilson, 2024] and inland seas emerged, which could have contributed to accelerated growth of biodiversity of marine biota in the II-year compared to terrestrial biota [Salles, 2023]. The high efficiency of mutagenesis involving ℵγ in nutrient medium of reservoirs was apparently combined in II-year with an increase in ℵγ flux density as the neutrino physics of Sun reached nominal level after ~200 Ma. By the beginning of Phanerozoic, the spiral structure of the Galaxy could also have stabilized [Zhang, 2017] and therefore tidal effects of stars on the SS acquired a regular character, repeating with a period of ~62 Myr in arms of the Galaxy. The strength of tidal effects could depend on oscillations of gravitational potential, as well as on changes in inclinations of Sun ~30° and the Earth ~60° (Fig. 9C). The gravitational potential decreases with increasing distance from the plane of the Galaxy up and down and changes in the spiral arms and the media between them. Fluctuations in gravitational potential and changes in inclinations of Sun and planets, by analogy with Milankovitch cycle mechanism of 405 kyr [Kent, 2018], should cause variations in insolation of Earth with light and ℵγ with a period of ~62 Myr. In this case, the pendulum oscillations of SS up and down from plane of Galaxy are synchronized with transitions between sectors of spiral arms. Thus, by analogy with astronomical-biotic cycle of 405 kyr in SS, it can be assumed that tidal effects on the scale of Galaxy modulate, by Milankovitch mechanism, geochronology of Phanerozoic marine biota with a period of ~62 Myr [Rohde, 2005] and sea level with a period of 36 ± 1 Myr [Boulila, 2023].

The growth and decline waves on I-year geochronology will correspond to sections of SS trajectory above and below plane of Galaxy, respectively (Fig. 9B). At present, the SS is located in the Orion galactic arm, and point **3**, which denotes P-Tr extinction at end of I-year (Fig. 8, Fig. 9B), will also correspond to point of 6th extinction, which will apparently end II-year [Barnosky, 2011; Ceballos, 2015]. Due to the lack of reliable data on the structure and dynamics of the Galaxy [Churchwell, 2009], the results of computer modeling of the trajectories and time of SS in arms differ significantly among different authors [Filipović, 2013; Gies, 2019; Gillman, 2018; 2019]. With such diversity in the chronometry of SS motion in the Galaxy, the hypotheses about the responsibility of

cosmic rays and radiation background in arms for climate change and global extinctions do not inspire confidence and are disputed [Medvedev, 2007; Svensmark, 2018; Smith, 2019; Wieler, 2011].

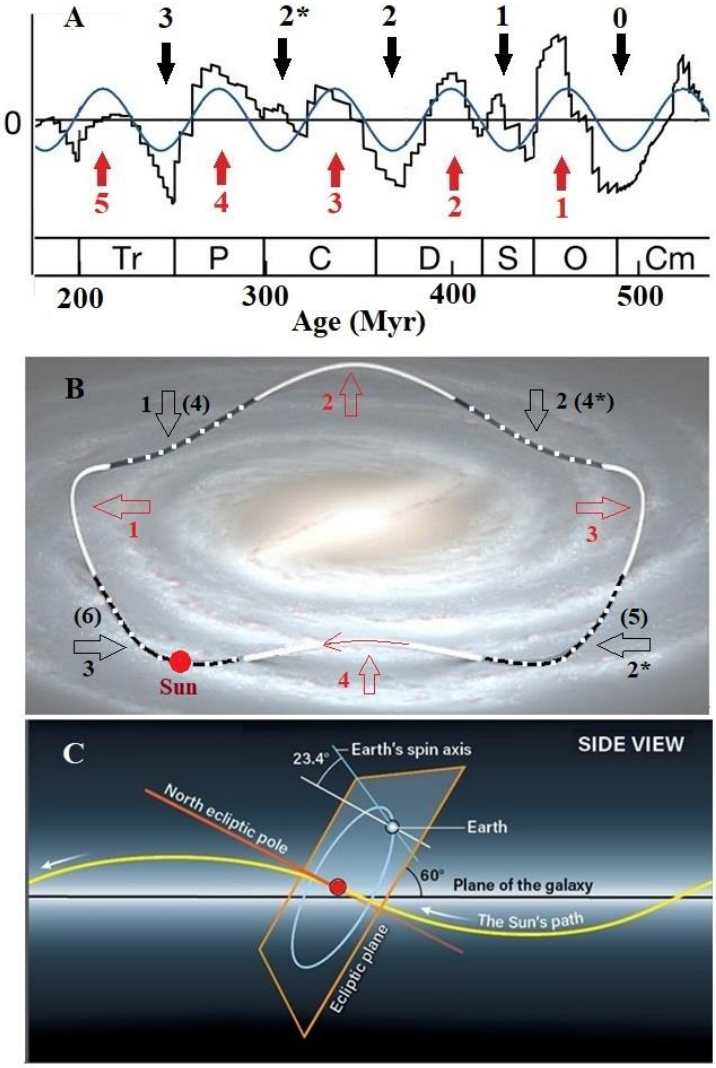

Fig. 9. A – approximation of the geochronology of marine biota by a sinusoidal wave with a period of 62 Myr and the separation of its maxima (red arrows) and minima (black arrows), **B** – wave orbit of Solar System around Galaxy with marking of extreme points from **1** to **4** from Fig. 8 in first galactic year (~500-250 Myr) and points of global extinctions from (**5**) to (**6**) in second year (~250-0 Myr). **C** – diagram of orientation of ecliptic of Solar System in motion along a wave orbit around center of Galaxy. Initial data for **A** from [Rohde, 2005], for **B** and **C** from [Klesman, 2020].

The following indirectly agrees with possibility of participation of cosmic ℵγ in thermodynamics of seas and mutagenesis. In [Kataoka, 2014], a connection was suggested between supernova explosions at about ~600 Ma and glaciation during the "Snowball Earth" period and the Cambrian explosion. Statistical analysis of the distribution of supernova explosions in arms of Galaxy showed an increase in their frequency over last ~510 Myr with a maximum in vicinity of ~280 Ma [Svensmark, 2018]. This result correlates with increase in P-Tr event of carbon-13 content in bottom sediments ($\delta^{13}C$ in Fig. 2) and with the doubling of marine invertebrate genera [Sepkoski, 2002].

3.5. The sixth global extinction and anthropogenesis

A significant difference between the 6th global extinction (6GEX) and the 3rd P-Tr extinction (3GEX) will be the addition of a biogenic factor associated with human activity to the effects of abiogenic factors of 3GEX on the biosphere. By now, the parasitism of human population on Earth's resources has led to average rate of loss of vertebrate species over last century already exceeding background rate of their extinction by ~100 times [Ehrlich, 2013; Ceballos, 2015]. Considering the reality of threat of loss of up to ~3/4 of biodiversity in the plant world due to global bee die-off, the International Union for Conservation of Nature initiated adoption of measures at regional and national levels to preserve bees as main pollinators [Byrne, 2009]. Against background of secular decline in T_G, climatic cataclysms and jumps in current T (0.025 °C/year, Fig. 3) [Pittock, 2009; Scafetta, 2023; Kristoufek, 2017] and CO_2 (2.5 ppm/year) [Carbon dioxide] have become more frequent. The growth of land T over past 50 years (Fig. 3) turned out to be four orders of magnitude faster than local jump in T_G at beginning of 3GEX (Fig. 1B, Fig. 2B, Fig. 3). At the same time, rate of increase in CO_2 concentration in 3GEX was 3 orders of magnitude higher than the growth rate of T_G (Fig. 2), and the growth of CO_2 over the past 50 years was 2 orders of magnitude faster than the jump in T (Fig. 3). Climatologists predict that due to the growth of T_G, changes in the circulation of ocean currents and the Gulf Stream could lead to a sharp decrease in T in Northern Europe in this century and plunge the Earth's climate into chaos [Open].

An analysis of the current state of the human ecosystem has allowed biologists and ecologists to call 6GEX «the suicide of civilization» [Sodhi, 2009; Barnosky, 2011; Kurzweil, 2014; Ceballos, 2015; Khlebodarova, 2020]. All five previous global extinctions of the Phanerozoic can be considered abiogenic corrections to the evolution of the biosphere. The extinctions in I-year contributed to the emergence of mammals, and the abiogenic factors of the extinctions in II-year adjusted the course of anthropogenesis up to the emergence of homo sapiens. By analogy with Le Chatelier's principle, 6GEX can be taken as a response of the biosphere aimed at neutralizing the negative impact of humans on it by initiating mutagenesis of their genome [Lynch, 2010]. As a result of the mutation, the «speech gene» [Enard, 2002] will be supplemented by the «gene mind», which is responsible for the dominance of the neurophysiology of thinking over the reproductive instinct [Pennisi, 2006; Kholmanskiy, 2012; 2019a; Kurzweil, 2014]. Since the changes in the physics of the Sun and the insolation of the Earth caused by the tidal effects of the galactic environment of the SS at the end of the II-year (Fig. 9B) are more pronounced in 6GEX than in 3GEX, then $\aleph\gamma$ can be proposed as the role of the mutagenic factor, the main target of which will be the chiral component of the mechanism of sexual reproduction.

The following evidence supports this assumption. The circadian and neuroendocrine rhythms of spermatogenesis and ovulation are regulated by the pineal hormone melatonin via the

hypothalamic-pituitary-gonadal axis [Frungieri, 2017; Heidarizadi, 2022, Khabarov, 2022]. Chiral metabolites are involved in the biosynthesis of melatonin in the pineal gland and male testicles, and its level in the blood plasma and brain ventricles changes synchronously with Аγ, reaching a maximum by 2-3 am [Kholmanskiy, 2019]. At the same time, a decrease in body T during sleep by ~1 °C, and in the testicles by 2 °C, promotes condensation of Аγ in the parenchyma of the pineal gland, testicles and in the HBs network of the cerebrospinal fluid [Kholmanskiy, 2023a].

Melatonin controls the biosynthesis of the hormone testosterone in male testicles [Penev, 2007; Frungieri, 2017]. In cells, testosterone is converted to a highly active metabolite, dihydrotestosterone, by adding a proton to the C5 carbon atom via the enzyme 5-alpha reductase. In this case, C5 becomes a chiral center, and its addition to the chiral centers C10, C13, C14 increases the sensitivity of dihydrotestosterone to Аγ. When the proton in the OH group in testosterone is replaced by a methyl group, the female sex hormone progesterone is obtained, which plays an important role in the regulation of female reproduction, including the mechanism of ribosome transcription. Thus, the key role of testosterone in the biochemistry of sexual reproduction allows for a wide range of mutations in the gene responsible for the production of the enzyme 5-alpha reductase [Labrie, 1992; Praveen, 2008]. The mutagenic effect of Аγ on the molecular mechanism of sexual reproduction can be associated, for example, with the birth of savants [Treffert, 2005]. Their unique mental abilities allow us to hope that the brain of modern man has all the prerequisites for reformatting anthropogenesis by the algorithms of the mind gene in the 6GEX period.

4. Conclusion

An illustration of possible involvement of sexual reproduction mutagenesis in 6GEX is the background mortality of honey bees [Byrne, 2009; Balvino-Olvera, 2023]. Laboratory studies at the University of Maryland, USA (39° N) have shown that over period from 1970 to 2019, the average lifespan of worker bees decreased from 34 to 17 days [Nearman, 2022]. Worker bees determine viability of the swarm, so a decrease in their number dooms the swarm to early extinction. These experiments were carried out at optimal T, excluding impact of pesticides, Varroa mites and technogenic electromagnetic radiation on bees. It follows that probable cause of reduction in the life and number of bees is a failure in genetic homeostasis program. Since worker bees are born from fertilized eggs, a genotype failure can occur due to participation of a mutant male chromosome in the formation of the zygote or due to a violation of complementarity between chiral elements in protein helices of male and female chromosomes. The generation of mutations and disorder in protein helices can be initiated by action of Аγ on the water-protein systems of cells with a disturbed water balance. This is indicated by the strong dependence of bee survival on quality and quantity of water used to water the bees in the experiment [Nearman, 2022]. The accumulation of mutations from the action of Аγ in bees will be facilitated by storage of entire sperm reserve (~6 million) in the spermatheca of the

queen during 2-7 years of her life. Note that the decrease in the number of bee colonies from 1990 to 2021 is dominant in countries above ~35° N. – Europe (-16%), North America (-9%), while in countries below ~35° N – Southern Europe (120%), South America (73%), Africa (47%), Asia (100%) their number increases [Bee colonies] may be together with honey acidity. The qualitative correlation of these changes with the demography of intellectual potential and population density above and below ~35° N [Nearman, 2022] is consistent with the hypothesis of participation of Ϡγ in mutagenesis of sexual reproduction and confirms dependence of intensity of Ϡγ flows emanating from the earth on the distribution of the water/land ratio at the local and planetary levels.

References

Annoni E. et al., (2024) Enhanced quantum transport in chiral quantum walks, Quantum Information Processing, 23(4) 10.1007/s11128-024-04331-y

Athar M. S. et al., (2022) Status and perspectives of neutrino physics, Prog. Part. Nucl. Phys. 124(1):103947, 10.1016/j.ppnp.2022.103947

Avdeeva, L.V. , Coltover, V.K. (2016) Nuclear spin catalysis in living nature. Bull. MSU. Ser. 2. Chemistry. 57(3) 145 http://www.chem.msu.su/rus/vmgu/163/145.pdf

Bachan A., Kump L. R. (2015) The rise of oxygen and siderite oxidation during the Lomagundi Event. PNAS. 112, 6562. 10.1073/pnas.142231911

Bahcall J.N., et al., (1982) Standard solar models and the uncertainties in predicted capture rates of solar neutrinos, Rev. Mod. Phys. 54(3):767, 10.1103/RevModPhys.54.767

Baguñà J. et al., (2008) Back in time: a new systematic proposal for the Bilateria, Philos. Trans. R. Soc. B. 363 (1496):1481. 10.1098/rstb.2007.2238

Balvino-Olvera F.J., et al. (2023) Long-term spatiotemporal patterns in the number of colonies and honey production in Mexico, Sci. Rep. 13, 1017. 10.1038/s41598-022-25469-8

Barnosky A., et al., (2011) Has the Earth's sixth mass extinction already arrived?. Nature, 471, 51. 10.1038/nature09678

Beckman I. N. Nuclear Medicine: Physical and Chemical Foundations, 400 (2024) https://urait.ru/index.php/bcode/538211

Bee colonies: Worldwide population on the rise, Estimates FAO (Crops and livestock products/ Live animals) https://www.destatis.de/EN/Themes/Countries-Regions/International-Statistics/Data-Topic/AgricultureForestryFisheries/Bees.html

Bloom B.P. et al., (2017) Chirality control of electron transfer in quantum dot assemblies. J. Am. Chem. Soc. 139: 9038, 10.1021/jacs.7b04639.

Boag T.H. et al., (2018) Oxygen, temperature and the deep-marine stenothermal cradle of Ediacaran evolution, Proceed. Royal Society B, 285(1893) 20181724, 10.1098/rspb.2018.1724

Borexino Collaboration. (2018) Comprehensive measurement of *pp*-chain solar neutrinos. Nature, 562, 505. 10.1038/s41586-018-0624-y

Boulila S. et al., (2021) Potential encoding of coupling between Milankovitch forcing and Earth's interior processes in the Phanerozoic eustatic sea-level record, Earth-Science Rev. 220(12):103727, 10.1016/j.earscirev.2021.103727

Boulila S. et al., (2023) Earth's interior dynamics drive marine fossil diversity cycles of tens of millions of years, PNAS 120(29) 1. 10.1073/pnas.222114912019. Boyd R.N., et al., Supernovae, neutrinos, and the chirality of the amino acids. Int. J. Mol. Sci. 12, 3432 (2011).

Brookes J.C. (2017) Quantum effects in biology: golden rule in enzymes, olfaction, photosynthesis and magnetodetection. Proc. R. Soc. A, 473: 20160822, 10.1098/rspa.2016.0822

Bulavin L.A. et al., (2023) Thermodynamic anomalies of water near its singular temperature of 42 °C, J. Mol. Liq. 122849, 10.1016/j.molliq.2023.122849

Burgess S.D., (2014) High-precision timeline for Earth's most severe extinction, Earth Atmospheric Planetary Sci. 111 (9) 3316. 10.1073/pnas.131769211

Butterfield N. J. (2007) Macroevolution and macroecology through deep time. Palaeontology. 50 (1): 41. 10.1111/j.1475-4983.2006.00613.x

Byrne A.W., Fitzpatrick Ú., (2009) Bee conservation policy at the global, regional and national levels, Apidologie, 40(3) 194, 10.1051/apido/2009017
Carbon dioxide in Earth's atmosphere, https://en.wikipedia.org/wiki/Carbon_dioxide_in_Earth%27s_atmosphere
Cauley P.W. et al. (2019) Magnetic field strengths of hot Jupiters from signals of star–planet interactions. Nat. Astron. 3, 1128. 10.1038/s41550-019-0840-x
Charbonneau P. (2022) External forcing of the solar dynamo, Front. Astron. Space. Sci. 9:853676, 10.3389/fspas.2022.853676
Churchwell, E., et al., (2009) The *Spitzer*/GLIMPSE Surveys: A New View of the Milky Way PASP 121, 213. https://iopscience.iop.org/article/10.1086/597811
Cionco, R.G., et al., (2023) Tidal Forcing on the Sun and the 11-Year Solar-Activity Cycle. Sol. Phys. 298, 70. 10.1007/s11207-023-02167-w
Daley A.C. (2019) A treasure trove of Cambrian fossils. Sci. 363(6433):1284. 10.1126/science.aaw864455.
Delgado E.A., et at, (2022) Probing neutrino decay scenarios by using the Earth matter effects on supernova neutrinos J. Cosmology Astroparticle Phys. (01):003, 10.1088/1475-7516/2022/01/003
Dolgov, A.D. Cosmology and neutrino properties. Phys. Atom. Nuclei, **71**, 2152 (2008). 10.1134/S1063778808120181
Dobretsov N.L. et al. (2008) On important stages of geosphere and biosphere evolution, in Book. Biosphere origin and evolution, Springer, 3, 10.1007/978-0-387-68656-1_1
Dvornyk V. et al., (2003) Origin and evolution of circadian clock genes in prokaryotes. PNAS. 100 (5): 2495. 10.1073/pnas.0130099100
Edwards C. et al., (2015) Paired carbon isotopic analysis of Ordovician bulk carbonate ($\delta^{13}C_{carb}$) and organic matter ($\delta^{13}C_{org}$) spanning the Great Ordovician Biodiversification Event, Palaeogeography, Palaeoclimatology, Palaeoecology, 458 10.1016/j.palaeo.2015.08.005
Ehrlich R., Ehrlich A., (2013) Can a collapse of global civilization be avoided? Proc. Biol. Sci. 280, 20122845. 10.1098/rspb.2012.2845
Eisenberg D. and Kauzman W., The structure and properties of water. L. 2007
Eguchi J. et al., (2019) Great Oxidation and Lomagundi events linked by deep cycling and enhanced degassing of carbon, Nature Geoscience. . 10.1038/s41561-019-0492-6
Enard, W. et al. (2002) Molecular evolution of *FOXP2*, a gene involved in speech and language. Nature, 418, 869, 10.1038/nature01025
Erlykin A.D., et al., (2017) Mass extinctions over the last 500 myr: an astronomical cause? Palaeontology. 60(2):159. 10.1111/pala.12283
Fan Y. (2021) Magnetic fields in the solar convection zone Living Reviews in Solar Physics, 18(5) 10.1007/s41116-021-00031-2
Fan J. (2020) A high-resolution summary of Cambrian to Early Triassic marine invertebrate biodiversity, Science, 367, 272. 10.1126/science.aax49
Fedonkin M.A. (2003) The origin of the Metazoa in the light of the Proterozoic fossil record, Paleontological Res. 7(1). 10.2517/prpsj.7.9
Filipović M. D. et al., (2013) Mass extinction and the structure of the milky way, Serb. Astron. J. 187, 10.2298/SAJ130819005F
Phillips L.F. (2014) Energy levels of neutrinos in a gravitational potential well, Appl. Phys. Res. 7(1) 10.5539/apr.v7n1p19
Fossat E. (2014) Asymptotic g modes: Evidence for a rapid rotation of the solar core, Astron. Astrophys. 604 (2014) 10.1051/0004-6361/201730460
Frungieri M.B. et al., (2017) Local Actions of Melatonin in Somatic Cells of the Testis. Int. J. Mol. Sci. 18:1170. 10.3390/ijms18061170
Gavelya E.A. Electric currents in the evolutionary transformation of the Earth, St. Petersburg, 2018. 150. https://fis.wikireading.ru/9058
Ceballos G., et al. (2015) Accelerated modern human-induced species losses: Entering the sixth mass extinction. Sci. Adv. 1(5) e1400253. 10.1126/sciadv.1400253
Gies D., Helsel J. (2019) Ice age epochs and the sun's path through the galaxy, Astrophys. J. 10(6), 2147
Gillman M.P. et al., (2018) Mapping the location of terrestrial impacts and extinctions onto the spiral arm structure of the Milky Way, Int. J. Astrobiol. 1. 10.1017/S1473550418000125
Gillman M., et al., (2019) Reconciling the Earth's stratigraphic record with the structure of our galaxy Geoscie. Front. 10.1016/J.GSF.2019.06.001

Giunti C., Studenikin A. (2015) Neutrino electromagnetic interactions: a window to new physics. Rev. Mod. Phys. 87.531, 10.1103/RevModPhys.87.531
Grandpierre A., Gustin Agoston G. (2005) On the onset of thermal metastabilities in the solar core. Astrophys Space Sci. 298, 537. 10.1007/s10509-005-5918-5
Glattfelder J.B. Volume II: The Simplicity of Complexity In book: Zum Performativen des frühen Dialogs, (2019) 10.1007/978-3-030-03633-1_6
Globus N., Blandford R.D., (2020) The chiral puzzle of life, ApJL, 895, L1, arXiv:1911.02525
Goldblatt C. et al., (2009) Nitrogen-enhanced greenhouse warming on early Earth. Nature Geosci, 2, 891. 10.1038/ngeo692
Goodman M. et al., (1990) Primate evolution at the DNA level and a classification of hominoids, J. Molecular Evolution, 30 (3). 260
Hady A.A., (2013) Deep solar minimum and global climate changes, J. Adv. Res. 4(3) 209 10.1016/j.jare.2012.11.001
Hady A. (2009) Descriptive study of solar activity sudden increase and Halloween storms of 2003, J. Atmos. Solar. Terr. Phys. 71, 1711, 10.1016/j.jastp.2008.11.019
Harmon L. J. et al., (2021) Causes and consequences of apparent time scaling across all estimated evolutionary rates. Annu. Rev. Ecol. Evol. Syst. 52, 587, 10.1146/annurev-ecolsys-011921-023644
Heidarizadi S. et al., (2022) Overview of biological effects of melatonin on testis: A review. Andrologia. 54(11): 14597. https://doi.org/10.1111/and.14597
Hotta H., et al, (2021) Solar differential rotation reproduced with high-resolution simulation. Nat. Astron. 5, 1100. 10.1038/s41550-021-01459-0
Horstmann G., et al., (2023) Tidally forced planetary waves in the tachocline of solar-like stars. Astrophys. J. 944, 48. 10.3847/1538-4357/aca278
Hinnov L.A. (2018) Astronomical metronome of geological consequence, PNAS, 115 (24) 6104 10.1073/pnas.1807020115
Hori K., et al. (2023) Jupiter's cloud-level variability triggered by torsional oscillations in the interior. Nat. Astron. **7**, 825. 10.1038/s41550-023-01967-1
Hoyle F., (1975) A Solar model with low neutrino emission, Astrophys. J. (Lett.), 197, L127. https://adsabs.harvard.edu/pdf/1975ApJ...197L.127H
Isozaki Y. et al. (2014) Beyond the cambrian explosion: From galaxy to genome, Gondwana Res. 25(3) 881. 10.1016/j.gr.2014.01.001
Jupiters Orbit, https://flight-light-and-spin.com/n-body/jupiter.htm
Kataoka R. et al., (2014) The Nebula Winter: The united view of the snowball Earth, mass extinctions, and explosive, Gondwana Res. 25(3):115. 310.1016/j.gr.2013.05.003
Kent D.V. et al., (2018) Empirical evidence for stability of the 405-kiloyear Jupiter–Venus eccentricity cycle over hundreds of millions of years, PNAS, 115 (24) 6153 10.1073/pnas.1800891115
Khabarov CV, Sterlikova ON. (2022) Melatonin and its role in circadian regulation of reproductive function. Vestnik novih medicinskih tehnologii. 29(3):17. https://doi.org/10.24412/1609-2163-2022-3-17-31
Khlebodarova T.M., Likhoshvai V.A. (2020) Causes of global extinctions in the history of life: facts and hypotheses. Vavilov J. Genetics and Breeding. 24(4) 407, 10.18699/VJ20.633
Kholmanskiy A., (2023) Role of water in physics of blood and cerebrospinal fluid, arXiv:2308.03778
Kholmanskiy A. (2023a) Connection of brain glymphatic system with circadian rhythm, bioRxiv 10.1101/2023.08.07.552123
Kholmanskiy A. (2021), Synergism of dynamics of tetrahedral hydrogen bonds of liquid water Phys. Fluids 33(6):067120, 10.1063/5.0052566
Kholmanskiy A. (2020) Spirit and matter, J. Herald Russian Spirit, 10, https://viewer.rsl.ru/ru/rsl01011376855?page=7&rotate=0&theme=white
Kholmanskiy A., (2019) Dialectic of Homochirality. Preprints, 2019060012, https://www.preprints.org/manuscript/201906.0012/v1
Kholmanskiy A. Biology and Demography of Creative Potential. Preprints (2019a), 10.20944/preprints201907.0198.v1
Kholmanskiy A.S. (2017) Structure of nucleus and periodic law of Mendeleev. Electron. Math. Med.-Biol. J. 16(1) 10.20944/preprints201906.0027.v1
Kholmanskiy A. (2016) Chirality anomalies of water solutions of saccharides. JML, 216, 683. 10.1016/j.molliq.2016.02.006
Kizel', V. A. Physical causes of dissymmetry of living systems, 1985, 120

Klesman A., (2020) In which direction does the Sun move through the Milky Way? Astronomy 6, https://www.astronomy.com/science/in-which-direction-does-the-sun-move-through-the-milky-way/
Knapp B.D., Huang K.C., (2022) The effects of temperature on cellular physiology, Ann. Rev. Biophys. 51, 499 10.1146/annurev-biophys-112221-074832
Kristoufek L. (2017) Has global warming modified the relationship between sunspot numbers and global temperatures? Phys. A Stat. Mechanics and its Applications 468, 351, 10.1016/j.physa.2016.10.089
Kurzweil R., (2014) The Singularity Is Near, In book: Ethics and Emerging Technologies, 10.1057/9781137349088_26;
Labrie F. (1992) Structure of human type-ii 5-alpha-reductase gene, Endocrinology 131(3):1571. 10.1210/en.131.3.1571
Laskar J. et al., (2011) La2010: A new orbital solution for the long-term motion of the Earth. Astron. Astrophys. 532, 81. 10.1051/0004-6361/201116836
Li X., et., (2020) Quantum transport on large-scale sparse regularnetworks by using continuous-time quantum walk. Quantum Inf. Process. 19(8), 235. 10.1007/s11128-020-02731-4
Liu M., et al., (2015) Supramolecular chirality in self-assembled systems, Chem. Rev. 115, 15, 7304. 10.1021/cr500671p
Langmuir C. H., Broecker W., How to build a habitable planet, Princeton University Press, Princeton, NJ 08540, (2012). https://www.habitableplanet.org/lecture-powerpoints
Lupovitch J. (2004) In The blink of an eye: how vision sparked the big bang of evolution, Arch. Ophthalmol. 124(1):142. 10.1001/archopht.124.1.142
Lyons T., et al., (2014) The rise of oxygen in Earth's early ocean and atmosphere. Nature, 506, 307. 10.1038/nature13068
Livshits I., Obridko V.N., (2006) Variations of the dipole magnetic moment of the Sun during the solar activity cycle, Astronomy Reports, 50(11): 926, 10.1134/S1063772906110060
Leamon R. J. et al., (2022) Deciphering Solar Magnetic Activity: The Solar Cycle Clock. Front. Astronomy Space Sci. 9:886670, 10.3389/fspas.2022.886670
Leong S. Period of the Sun's Orbit around the Galaxy (Cosmic Year). Phys. Factbook (2002).
Lynch M. (2010) Rate, molecular spectrum, and consequences of human mutation, PNAS, 107(3) 961. 10.1073/pnas.0912629107
Magnetic dipoles of the Sun and planets, https://www.physicsforums.com/threads/dipole-moments-of-the-planets-and-the-sun.268157/
Manda S. et al., (2020) Sunspot area catalog revisited: Daily cross-calibrated areas since 1874, Astron. Astrophys. 640 A78, 10.1051/0004-6361/202037547
Mann M. et al., (1999) Northern hemisphere temperatures during the past millennium: Inferences, uncertainties, and limitations, Geophys. Res. Let. **26** (6): 759, 10.1029/1999GL90007060.
Markov A.V. (2009) Origin and evolution of man. Review of achievements of paleoanthropology, genetics, evolutionary psychology. Report. https://evol-biol.ru/document/922
Matyushin G.N. Three Million Years BC. Moscow: 1986. 155; https://search.rsl.ru/ru/record/01001325394
Medvedev M.V., (2010) "Evaporation" of a flavor-mixed particle from a gravitational potential, J. Phys. A: Math. Theor. 43(37) 10.1088/1751-8113/43/37/372002
Medvedev M.V., Melott A.L., (2007) Do extragalactic cosmic rays induce cycles in fossil diversity? Astr. J. 664(2) 10.1086/518757
Melott A.L., Bambach R.K., (2010) A ubiquitous ~62-Myr periodic fluctuation superimposed on general trends in fossil biodiversity. I. Documentation, Paleobiology 37(1) 92. https:arxiv.org/pdf1005.4393
Melott A.L., Bambach R.K., (2010a) A ubiquitous ~62 Myr periodic fluctuation superimposed on general trends in fossil biodiversity: II, Evolutionary dynamics associated with periodic fluctuation in marine diversity. Paleobiology, 37 (3) 383 https://arxiv.org/pdf/1011.4496
Michel S., Meijer J.H., (2019) From clock to functional pacemaker, Eur. J. Neurosci, 51(1), 10.1111/ejn.14388
Milankovitch cycles, https://en.wikipedia.org/wiki/Milankovitch_cycles
Maltoni M., Smirnov A.Yu., (2016). Solar neutrinos and neutrino physics. Eur. Phys. J. A, 52, 87. 10.1140/epja/i2016-16087-0
Mishra S. et al., (2020) Length-dependent electron spin polarization in oligopeptides and DNA. J. Phys. Chem. 124:10776, 10.1021/acs.jpcc.0c02291
Muñoz-Jaramillo A., (2009) Helioseismic data inclusion in solar dynamo models. Astrophysical J, 698(1):461. 10.1088/0004-637X/698/1/461

Muñoz-Jaramillo A. et al., (2010) A double-ring algorithm for modeling solar active regions: unifying kinematic dynamo models and surface flux-transport simulations, Astrophys. J. Let. 720 L20, 10.1088/2041-8205/720/1/L20
Naaman R., et al., (2022) Chiral induced spin selectivity and its implications for biological functions, Ann. Rev. Biophys. 51, 99, 10.1146/annurev-biophys-083021-07040096.
Nandy D. et al. (2021) Solar evolution and extrema: current state of understanding of long-term solar variability and its planetary impacts. Prog. Earth. Planet. Sci. 8, 40. 10.1186/s40645-021-00430-x
Nataf H.C. (2022) Tidally Synchronized Solar Dynamo: A Rebuttal. Sol. Phys. 297, 107. 10.1007/s11207-022-02038-w
Nataf H.C. (2023) Response to Comment on "Tidally Synchronized Solar Dynamo: A Rebuttal". Sol Phys, 298, 33. 10.1007/s11207-023-02128-3
Nearman A., Engelsdorp D. (2022) Water provisioning increases caged worker bee lifespan and caged worker bees are living half as long as observed 50 years ago, Sci. Rep. 12, 18660. 10.1038/s41598-022-21401-2
Okhlopkov, V.P. (2020) 11-Year Index of Linear Configurations of Venus, Earth, and Jupiter and Solar Activity. Geomagn. Aeron. 60, 381. 10.1134/S0016793220030147
Open Letter by Climate Scientists to the Nordic Council of Ministers Reykjavik, October 2024 https://en.vedur.is/media/ads_in_header/AMOC-letter_Final.pdf
Osozawa S. (2023) Geologically calibrated mammalian tree and its correlation with global events, including the emergence of humans, Ecol. Evol. 13(12) e10827. 10.1002/ece3.10827
Palin R.M. et al., (2020) Secular change and the onset of plate tectonics on Earth, Earth-Sci. Rev. 207. 10.1016/j.earscirev.2020.103172
Parmon, V.N., (2008) The prebiotic phase of the origin of life as seen by a physical chemist. In: Biosphere Origin and Evolution. Springer, Boston, 10.1007/978-0-387-68656-1_6
Payne J.L., Clapham M.E., (2012) End-Permian mass extinction in the oceans: An ancient analog for the twenty-first century? Annu. Rev. Earth Planet. Sci. 40, 89. 10.1146/annurev-earth-042711-105329
Penev P.D. (2007) Association between sleep and morning testosterone levels in older men. Sleep. 30(4): 427-43217520786 Google Scholar
(2006) Pennisi E. Mining the molecules that made our mind, Sci. 313. 1908 10.1126/science.313.5795.1908
Picoreti R. et al., (2016) Neutrino decay and solar neutrino seasonal effect, Phys. Lett. B, 761, 70 [arXiv:1506.08158].
Pipin V.V. (2014) Reversals of the solar magnetic dipole in the light of observational data and simple dynamo models, Astr. Astrophys. 567. 10.1051/0004-6361/201323319
Planavsky N.J., (2021) Evolution of the structure and impact of Earth's biosphere. Nat. Rev. Earth Environ, 2, 123. 10.1038/s43017-020-00116-w
Pittock B. (2009) Can solar variations explain variations in the Earth's climate? Climatic Change, 96, 483. 10.1007/s10584-009-9645-8
Praveen E.P. et al., (2008) Gender identity of children and young adults with 5-alpha-reductase deficiency. J Pediatr. Endocrinol. Metab. 21(2) 173, 10.1515/jpem.2008.21.2.173
Rohde R., Muller R. (2005) Cycles in fossil diversity. Nature, 434, 208. 10.1038/nature03339
Rolland J. et al., (2023) Conceptual and empirical bridges between micro- and macroevolution Nat Ecol Evol, 7(8) 1181, 10.1038/s41559-023-02116-7
Rozenman G.G. et al., (2018) Long-Range Transport of Organic Exciton-Polaritons Revealed by Ultrafast Microscopy. ACS Photonics. 5 (1): 105. 10.1021/acsphotonics.7b01332
Salles T., et al., (2023) Landscape dynamics and the Phanerozoic diversification of the biosphere, Nature. 624(7990) 115. 10.1038/s41586-023-06777-z
Scafetta N., (2023) Empirical assessment of the role of the Sun in climate change using balanced multiproxy solar records, Geosci. Front. 14(5):101650. 10.1016/j.gsf.2023.101650
Schirber M. (2014) Focus: Neutrinos are brighter at night, Physics, 7, 24, https://physics.aps.org/articles/v7/24
Schneider N. M., Bagenal F. (2007) Io's neutral clouds, plasma torus, and magnetospheric interactions, 265. 10.1007/978-3-540-48841-5_11 .
Scotese C.R. et al., (2021) Phanerozoic paleotemperatures: The earth's changing climate during the last 540 million years, Earth-Sci. Rev. 215, 103503. 10.1016/j.earscirev.2021.103503
Seker I. (2013) Are planetary tides on the sun and the birthplace of sunspots related? Solar Physics 286(2) 10.1007/s11207-013-0288-6
Sepkoski J.J. (1984) A kinetic model of Phanerozoic taxonomic diversity. III. Post-Paleozoic families and mass extinctions. Paleobiology, 10, 246. 10.1017/s0094837300008186

Sepkoski J. J. Jr. (1997). Biodiversity: Past, Present, and Future. J. Paleontology, 71(4), 533, 10.1017/s0022336000040026
Sepkoski, J.J. (2002) A compendium of fossil marine animal genera. Bull. Am. Paleont., 363, 1–560.
Shaviv N. J. (2008) Using the oceans as a calorimeter to quantify the solar radiative forcing, J. Geophys. Res., 113, A11101, 10.1029/2007JA012989
Shimkevich A.L., Shimkevich I.Y., (2011) On water density fluctuations with helices of hydrogen bonds, Adv. Condens. Matt. Phys. ID 871231, 5, 10.1155/2011/871231
Singh S.K. et al., (2012) Wireless transmission of electrical power overview of recent research & development, Int. J. Comp. Electrical Engineering, 4(2) http://ijcee.org/papers/480-N015.pdf
Sivaraman K.R., (2010) Are Polar Faculae Generated by a Local Dynamo? Astrophys. Space Sci. Proceed. 386. 10.1007/978-3-642-02859-5_36
Smith A.B., McGowan A. J., (2005) Cyclicity in the fossil record mirrors rock outcrop area, Bio. Lett. 1(4) 443 10.1098/rsbl.2005.0345
Smith A.B. (2007) Marine diversity through the Phanerozoic: problems and prospects, J. Geo. Society, 164(4) 731. 10.1144/0016/76492006-184
Smith T., (2019) The constancy of galactic cosmic rays as recorded by cosmogenic nuclides in iron meteorites Meteoritics & Planetary Sci. 54(12) 10.1111/maps.13417
Sodhi N.S., et al., **(**2009) Causes and consequences of species extinctions, In book: The Princeton Guide to Ecology, Chapter: 1, 10.1515/9781400833023.514
Song H., Scotese C.R., (2023) The end-Paleozoic great warming, Sci. Bulletin, 68(21) 2523 10.1016/j.scib.2023.09.009
Song, H., et al, (2019) Seawater temperature and dissolved oxygen over the past 500 million years, J. Earth Sci. 30(2). 236. 10.1007/s12583-028-1002-2
Sorokhtin, O.G., et al., Theory of Earth Development (Origin, Evolution and Tragic Future). Institute Computer Studies, Izhevsk, 751. (2010)
Space Weather, https://www.spaceweatherlive.com/en/solar-activity/solar-cycle.html
Spencer C.J. et al. (2018) A Palaeoproterozoic tectono-magmatic lull as a potential trigger for the supercontinent cycle. Nature Geosci, 11, 97. 10.1038/s41561-017-0051-y
Stefani F. et al., (2019) A Model of a tidally synchronized solar dynamo. Sol Phys, 294, 60. 10.1007/s11207-019-1447-1
Stefani F. et al, (2024) Rieger, Schwabe, Suess-de Vries: The Sunny Beats of Resonance, Solar Physics, Solar Physics 299(4) 10.1007/s11207-024-02295-x
Sun Y. et al., (2012) Lethally hot temperatures during the Early Triassic greenhouse. Science, 338, 366. 10.1126/science.1224126
Svensmark H., (2012) Evidence of nearby supernovae affecting life on Earth, Mon. Not. R. Astron. Soc., 423, 1234, 10.1111/j.1365-2966.2012.20953.x
Treffert D.A, Christensen D.D. (2005) Inside the mind of a savant. Scientific American, 1, 10.1038/scientificamericanmind0606-50
de Toma G., et al. (2009) Solar cycle 23: an unusual solar minimum? AIP Conf Proc, 1216, 667. 10.1063/1.3395955
Tverdislov V.A., Malyshko E. V. (2020) Chiral dualism as an instrument of hierarchical structure formation in molecular biology, Symmetry 12(4):587, 10.3390/sym12040587 tesla
Impact events on Jupiter, https://en.wikipedia.org/wiki/Comet_Shoemaker–Levy_9
Vita-Finzi C., (2022) Sunspot periodicity, 10.48550/arXiv.2212.03249
Vidotto A.A. et al., (2018) The magnetic field vector of the Sun-as-a-star – II. Evolution of the large-scale vector field through activity cycle 24, MNRAS. 480 (1), 477, 10.1093/mnras/sty1926
Vorontsov S.V., Zharkov V.N. (1981) Free oscillations of the sun and the giant planets, Sov. Phys. Usp. 24, 697, 10.1070/PU1981v024n08ABEH004837
Valentine J., Moores E., (1970) Plate-tectonic regulation of faunal diversity and sea level: a model. Nature, 228, 657. 10.1038/228657a0
Wang G. et al., (2019) The end-Ordovician mass extinction: A single-pulse event? Earth-Sci. Rev., 192, 15, 10.1016/j.earscirev.2019.01.023
Westerhold T. et al., (2020) An astronomically dated record of Earth's climate and its predictability over the last 66 million years, Science. 369(6509) 1383. 10.1126/science.aba6853
Wieler R. et al., (2011) The galactic cosmic ray intensity over the past 10^6–10^9 years as recorded by cosmogenic nuclides in meteorites and terrestrial samples, Space Sci. Rev. 176, 351

Wilson I. R., (2013) The Venus-Earth-Jupiter spin-orbit coupling model, Pattern Recognition in Phys. 1(1):147, 10.5194/prp-1-147-2013
Wilson C. J., (2024) Unveiling the underlying drivers of Phanerozoic marine diversification, Proceed. Roy. Socie. B, 291, 20240165, 10.1098/rspb.2024.0165
Zaitseva N.V, et al., (2016) Dependence of the optical activity of solutions of terpenes and sugars on temperature. Bull. Moscow State Regional University. 1. 57, 10.18384/2310-7189-2016-1-57-63
Zhang X., Shu D., (2013) Causes and consequences of the Cambrian explosion, Sci. China Earth Sci. 57(5):930. 10.1007/s11430-013-4751-x
Zhang X. (2017) On a possible giant impact origin for the colorado plateau. arXiv:1711.03099
Zhang X.L. et al., (2014) Triggers for the Cambrian explosion: Hypotheses and problems. Gondwana Res. 25 (3), 896. 10.1016/j.gr.2013.06.001
Zerbo J.-L., et al. (2013) Geomagnetism during solar cycle 23: Characteristics, J. Adv. Res. 4(3) 265 10.1016/j.jare.2012.08.010